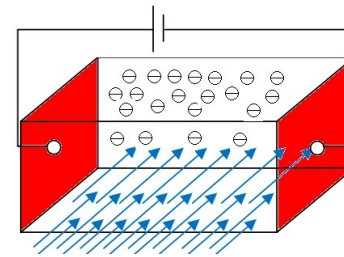
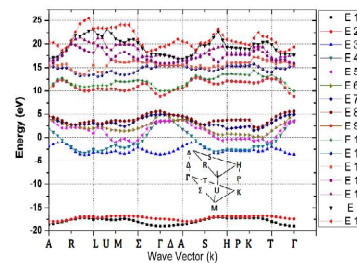
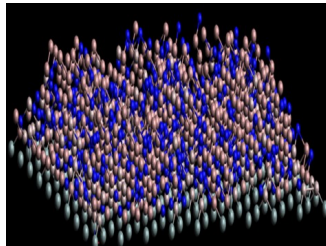




Material Growth, Characterization of III-V & II-VI Compounds and Various Device Applications

By
Dr. Praveen K Saxena



CRYSTAL GROWTH



Epitaxial Growth of Group IV, III-V & II-VI Semiconductors



CRYSTAL GROWTH



SILICON

- Available in up to >30 cm diameter
- Quite inexpensive and high quality
- Can be obtained n -type, p -type, or with high resistivity
- Used for Si and SiGe technologies
- Intense research to develop Si-based "pseudo-substrates" for GaAs, InP, CdTe...technologies

GaAs

- Available in up to >12 cm diameter
- High quality, more expensive than Si, but affordable
- Used for GaAs and AlGaAs, and strained InGaAs technologies
- Can be used for electronic and optoelectronic applications

InP

- 10 cm diameter available, but expensive
- InP and InGaAsP technologies can be grown
- Very important for optoelectronics and high performance electronics

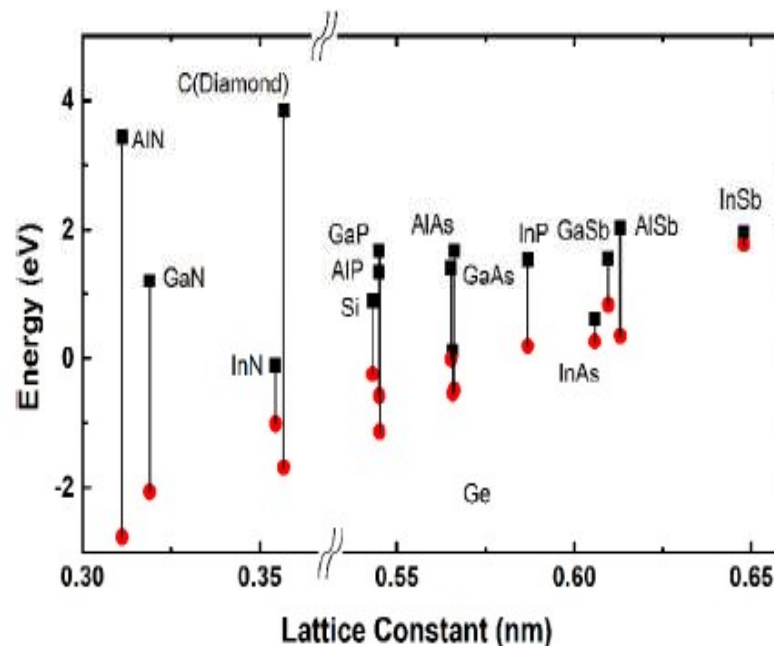
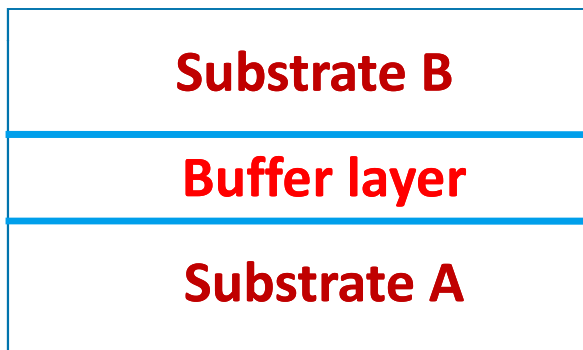
SiC

- Small, very expensive substrates
- Very important for high power, large gap technologies
- Used for nitride technology

EPITAXIAL GROWTH CHALLENGES



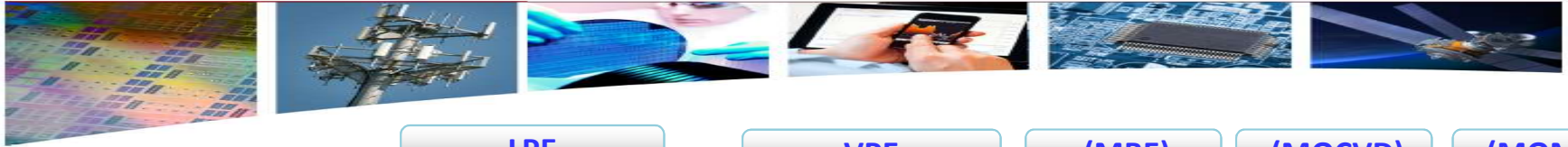
□ Development of psuedo-substrates



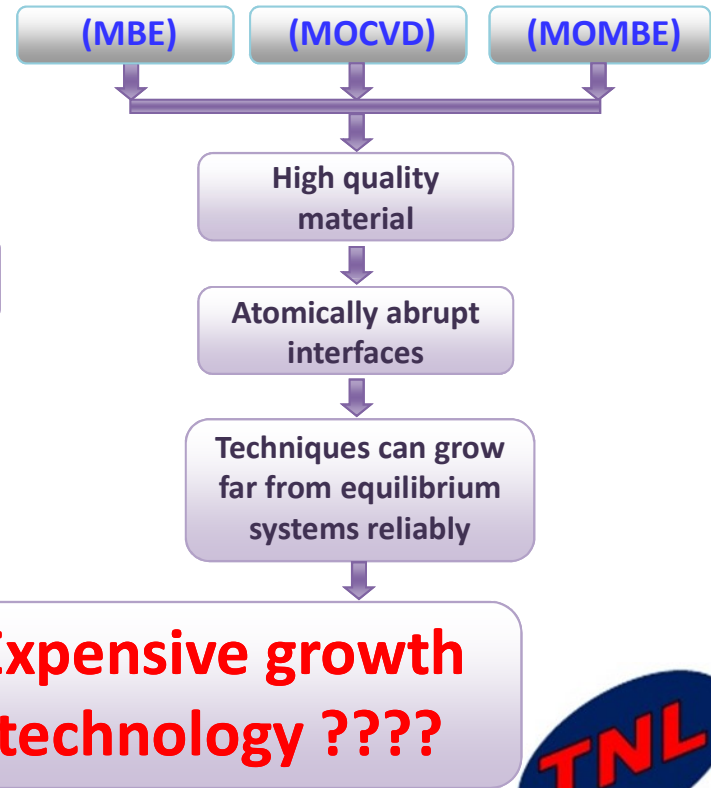
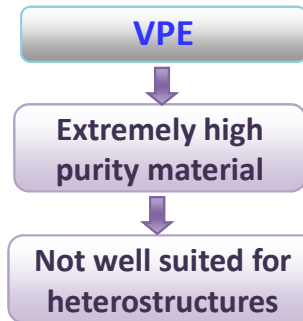
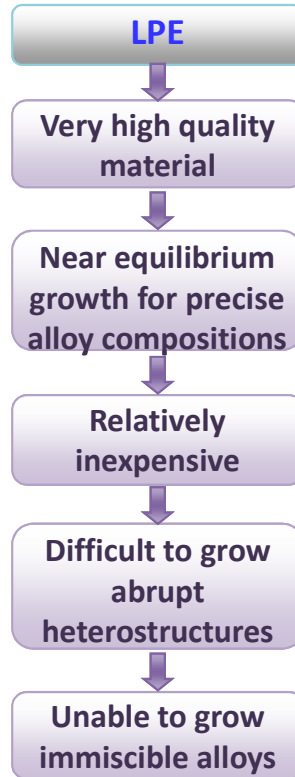
*E.T. Yu, J.O. McCaldin, T.C. McGill, Band offsets in semiconductor heterojunctions, in: E. Henry, T. David (Eds.), Solid State Physics, Academic Press, 1992, pp. 1-146



CRYSTAL GROWTH TECHNIQUES



Epitaxial Growth
 Semiconductor technologies dependent on non ideal substrates
 Lot of Technological Challenges



EPITAXIAL GROWTH CHALLENGES



- Multi components growth
- Point defects, e.g. vacancies, interstitial atoms
- Extended defects (dislocations & stacking faults)
- Dislocations reduce or relax strain

E.g. GaN growth

Substrate	Si	Al ₂ O ₃	SiC	Bulk GaN	AlN
Lattice Mismatch (%)	17	16	3.4	-	2.5
Thermal Conductivity (W/mm-k)	150	35	490	260	319
Resistivity (ohm-cm)	10 ⁴	10 ¹⁴	~10 ¹²	-	>10 ¹⁴

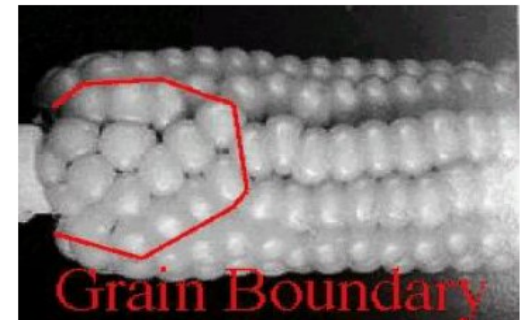
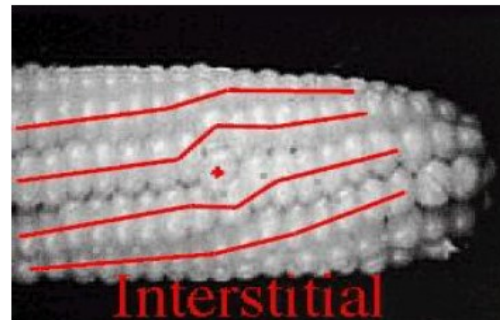
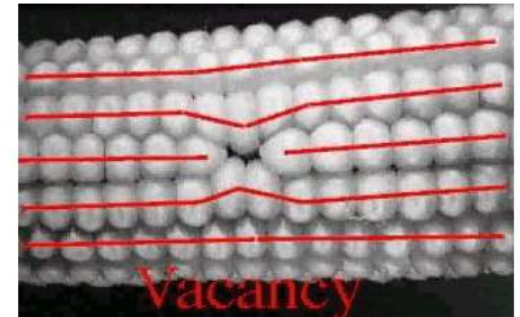
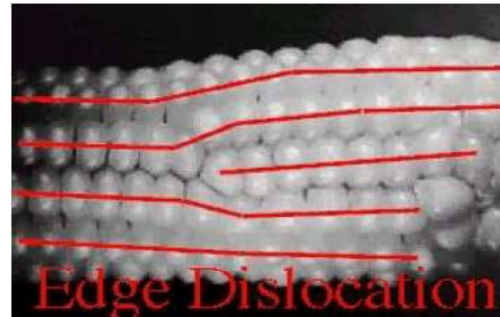


EPITAXIAL GROWTH CHALLENGES



Defects

- Edge Dislocation
- Vacancies
- Interstitial
- Grain Boundaries



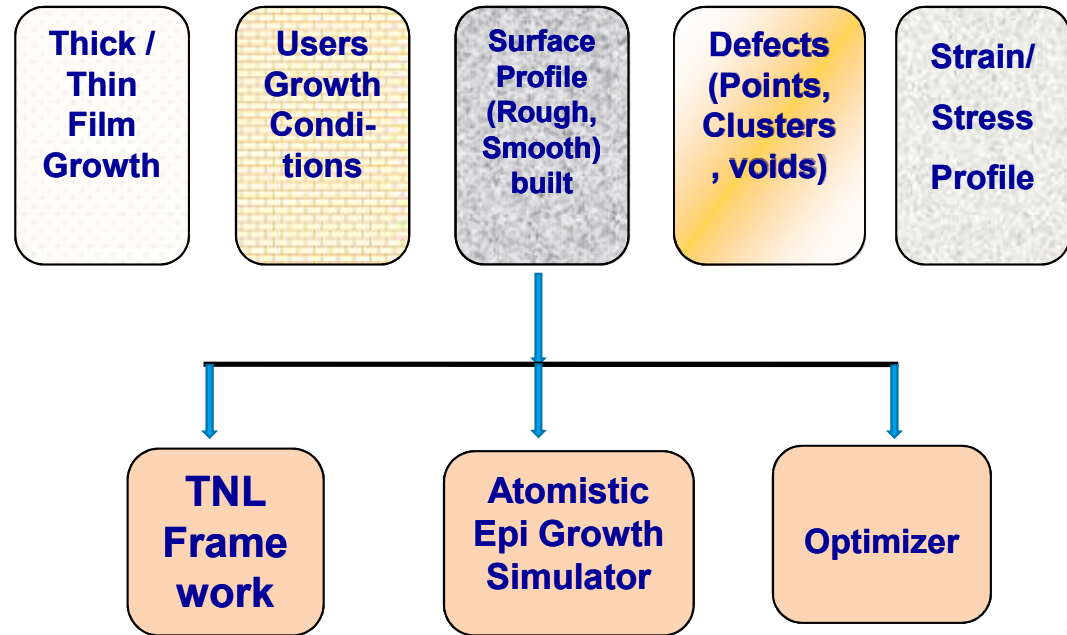
EpiGrow Simulator



Innovative Atomistic Reactor Simulation

Inbuilt Reactors

- MBE
- MOCVD
- GasMBE
- CVD & PVD (under development)

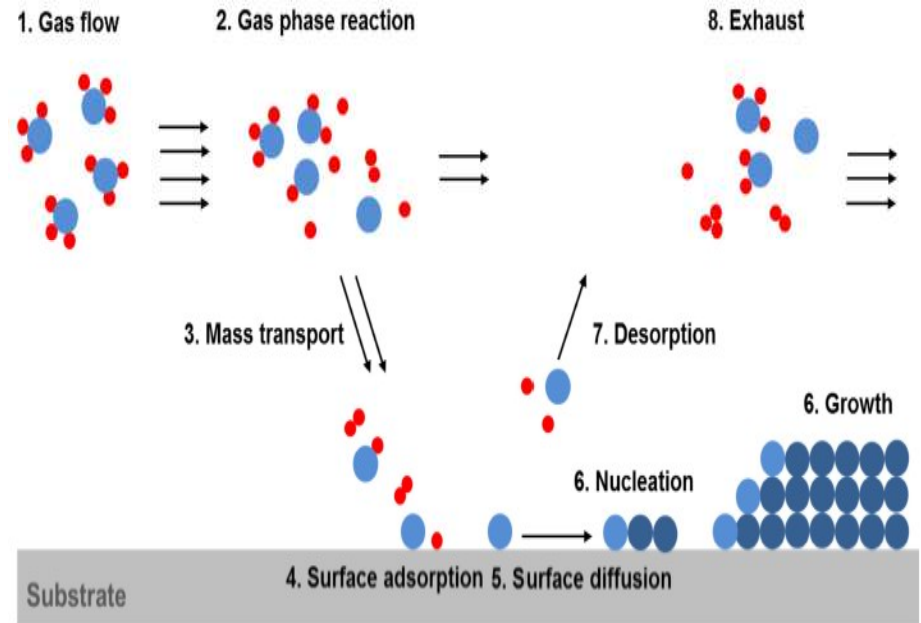


EpiGrow Simulator



Benefits can be realized

- Users growth conditions
- Surface profiles Extracting Roughness
- Defects Extraction (point/clusters)
- Extraction of dislocations & Stress/Strain
- Fewer experiments for optimization
- Reduction in waste during experimentation
- Ability to deal with different reactive species and reactor geometries
- On-line process control



EpiGrow Simulator



❑ **Schwoebel barrier:** The atom diffuses from the site exactly above the edge atom to the site immediately next to the edge atom,

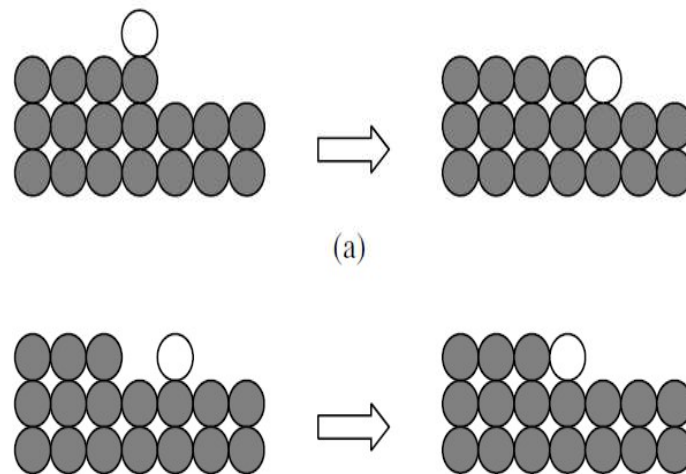
❑ **Incorporation barrier:** The atom incorporates into the edge on the same surface level.

❑ **Strain:** → $(a - a_0) / a_0$

❑ **Sticking coefficient** → $s_C = P_{ads}(1 - m) \sum_{n=0}^{\infty} P_{hop}^n$

❑ **Total Rates** $R_T = R_{ads} + R_{hop} + R_{des}$

Here ads ~ adsorption Rate on substrate , Hop ~ hopping rate on substrate
Des ~ desorption rate



Side view for the case of Schwoebel barrier (a) and that of incorporation barrier (b), where the white atom is the diffusing one.



GaAs/GaN: MOCVD EpiGrowth



Gas-phase Mechanisms:

					$k = AT^n e^{-E_a/RT}$	A	n	E_a	
G1	TMG	=	DMG	+ CH ₃		1.00×10^{47}	-9.18	76,996	
G2	DMG	=	MMG	+ CH ₃		7.67×10^{43}	-9.8	34,017	
G3	MMG	=	Ga	+ CH ₃		1.68×10^{30}	-5.07	84,030	
G4	TMG	+	NH ₃	→ TMG:NH ₃		2.28×10^{34}	-8.31	3115	
G5	TMG	+	NH ₃	→ DMG:NH ₂	+ CH ₄	1.70×10^{14}	2	19,969	
G6	DMG	+	NH ₃	→ DMG:NH ₃		4.08×10^{31}	-7.03	3234	
G7	DMG	+	NH ₃	→ MMG:NH ₂	+ CH ₄	5.30×10^{15}	1.56	20,744	
G8	MMG	+	NH ₃	→ MMG:NH ₃		7.95×10^{24}	-5.21	2094	
G9	MMG	+	NH ₃	→ GaNH ₂	+ CH ₄	8.10×10^{15}	1.3	17,722	
G10	NH ₃	+	CH ₃	→ NH ₂	+ CH ₄	3.31×10^{13}	2.51	9859	
G11	CH ₃	+	H ₂	→ CH ₄	+ H	1.20×10^{12}	0	12,518	
G12	TMG	+	H	→ DMG	+ CH ₄	5.00×10^{13}	0	10,036	
G13	DMG	+	H	→ MMG	+ CH ₄	5.00×10^{13}	0	10,036	
G14	TMG:NH ₃	→	MMG	+ 2CH ₃	+ NH ₃	1.33×10^{44}	-8.24	77,791	
G15	CH ₃	+	H	→ M	+ NH ₃	2.40×10^{22}	-1	0	
G16	2CH ₃	=	C ₂ H ₆			2.00×10^{13}	0	0	
G17	2H	+	M	=	H ₂	+ M	2.00×10^{16}	0	0

Surface phase Mechanisms:

					Path 1, $k = AT^n e^{-E_a/RT}$	A	n	E_a	
1	MMG	+	N(S)	→	MMG(S)	1.16×10^{15}	2.98	0	
2	MMG(S)	→	MMG	+ N(S)		1.12×10^{14}	0.55	107,673	
3	NH ₃	+	MMG(S)	→	COMP1(S)	3.35×10^{17}	3.33	0	
4	COMP1(S)	→	NH ₃	+ MMG(S)		5.70×10^{13}	-0.16	8146	
5	MMG	+	COMP1(S)	→	CH ₄	+ COMP2(S)	1.23×10^{10}	3.22	23,446
6	NH ₃	+	COMP2(S)	→	COMP3(S)	3.35×10^{17}	3.33	0	
7	COMP3(S)	→	NH ₃	+ COMP2(S)		5.70×10^{13}	-0.161	8146	
8	MMG	+	COMP3(S)	→	CH ₄	+ COMP4(S)	1.23×10^{10}	3.22	23,446
9	NH ₃	+	COMP4(S)	→	COMP5(S)	3.35×10^{17}	3.33	0	
10	COMP5(S)	→	NH ₃	+ COMP4(S)		5.70×10^{13}	-0.161	8146	
11	COMP5(S)	→	CH ₄	+ RINGM1(S)		1.23×10^{17}	3.22	23,446	
12	Ga(S)	+	RINGM1(S)	→	RINGM2(S)	+ N(S)	3.35×10^{17}	3.33	0
13	RINGM2(S)	→	3H ₂	+ 3GaN(B)	+ Ga(S)	3.68×10^9	2.05	59,610	

Epi-Grow [Run Output]

Substrate

Orientation 100 111

Substrate Dimension

Reactor **Time Interval for Roughness Calculation**

Number of Steps

Surface Energy (eV) **Substrate Temperature (°C)**

Schwoebel Barrier (eV) **Time (Step 1)**

Incorporation Barrier (eV) **Nearest Neighbour Energy (eV)**

Desorption Barrier (eV)

Precursor source

Showerhead Dimension

Area (cm²)

Height (cm) MOCVD Parameters

Chamber Radius (cm)

Chamber Volume (L)



GaN: MOCVD EpiGrowth



Surface phase Mechanisms: PATH 2

Path 2, $k = AT^n e^{-E_a/RT}$				A	n	E_a		
14	CH ₃	+	Ga(S)	→	MMG(S)	1.76×10^9	1.39	0
15	MMG(S)	→	CH ₃	+	Ga(S)	4.54×10^{13}	0.0346	79,480
16	NH ₂	+	Ga(S)	→	NH ₂ (S)	3.17×10^8	1.83	0
17	GaNH ₂	+	N(S)	→	GaNH ₂ (S)	2.27×10^6	2.247	0
18	GaNH ₂ (S)	→	GaNH ₂	+	N(S)	4.83×10^{13}	0.614	83,881
19	COMPMM1(S)	→	CH ₄	+	GaNH ₂ (S)	1.49×10^{11}	0.609	25,950
20	MMG	+	GaNH ₂ (S)	→	COMPMM1(S)	1.16×10^5	2.98	0
21	NH ₂	+	COMPMM1(S)	→	COMPMM2(S)	3.35×10^7	3.33	0
22	COMPMM2(S)	→	CH ₄	+	COMPMM3(S)	1.49×10^{11}	0.609	25,950
23	MMG	+	COMPMM3(S)	→	COMPMM4(S)	1.16×10^5	2.98	0
24	NH ₂	+	COMPMM4(S)	→	COMPMM5(S)	3.35×10^7	3.33	0
25	COMPMM5(S)	→	CH ₄	+	RINGM1(S)	1.49×10^{11}	0.609	25,950
26	NH ₂ (S)	→	NH ₂	+	Ga(S)	1.45×10^{14}	0.09	59,786
27	COMPMM1(S)	→	MMG	+	GaNH ₂ (S)	1.00×10^{14}	0.55	42,819
28	COMPMM2(S)	→	NH ₂	+	COMPMM1(S)	5.70×10^{15}	-0.1	8146
29	COMPMM4(S)	→	MMG	+	COMPMM3(S)	1.00×10^{14}	0.55	42,819
30	COMPMM5(S)	→	NH ₂	+	COMPMM4(S)	5.70×10^{15}	-0.1	8146
31	Ga	+	N(S)	→	Ga(S)	1.00×10^{11}	1.5	0
32	Ga(S)	+	NH ₂ (S)	→	GaNH ₂ + Ga(S)	1.00×10^{29}	0	0
33	Ga(S)	→	Ga	+	N(S)	1.00×10^{13}	0	45,168
34	6CH ₃	+	RINGM2(S)	→	COM1(S)	7.55×10^7	2.31	0
35	COM1(S)	→	6CH ₃	+	RINGM2(S)	1.00×10^{15}	0.71	45,506
36	COM1(S)	→	6CH ₄	+	3GaN(B) + Ga(S)	4.00×10^{12}	0	49,675

Surface phase Mechanisms: PATH 3

Path 3, $k = AT^n e^{-E_a/RT}$				A	n	E_a		
37	TMG	+	N(S)	→	TMG(S)	1.16×10^5	2.98	0
38	NH ₂	+	TMG(S)	→	TCOM1(S)	3.35×10^7	3.33	0
39	TCOM1(S)	→	CH ₄	+	TCOM2(S)	1.49×10^{11}	0.609	32,785
40	Ga(S)	+	TCOM2(S)	→	TCOM3(S)	3.35×10^7	3.33	0
41	TCOM3(S)	→	2CH ₄	+	GaN(B) + Ga(S)	1.49×10^{11}	0.609	49,675
42	TMG(S)	→	TMG	+	N(S)	1.12×10^{14}	0.55	49,675
43	TCOM1(S)	→	NH ₂	+	TMG(S)	5.70×10^{15}	-0.161	11,922
44	TMG:NH ₂	+	N(S)	→	TCOM1(S)	1.16×10^5	2.98	0
45	TCOM1(S)	→	TMG:NH ₂	+	N(S)	1.12×10^{14}	0.55	49,675
46	TCOM1(S)	→	2CH ₃	+	MMG(S) + NH ₃ + N(S)	1.12×10^{14}	0.55	10,7673
47	MMGNH ₃	+	N(S)	→	COMPMM1(S)	1.16×10^5	2.98	0
48	COMPMM1(S)	→	MMG:NH ₃	+	N(S)	1.12×10^{14}	0.55	107,673
49	MMG:NH ₃	+	COMPMM1(S)	→	CH ₄ + COMPMM3(S)	1.23×10^{10}	3.22	23,446
50	MMG:NH ₃	+	COMPMM3(S)	→	CH ₄ + COMPMM5(S)	1.23×10^{10}	3.22	23,446
51	MMG:NH ₃	+	GaNH ₂ (S)	→	COMPMM2(S)	1.16×10^5	2.98	0
52	MMG:NH ₃	+	COMPMM3(S)	→	COMPMM5(S)	1.16×10^5	2.98	0

Chemical Composition of compound on the surface

Compounds Names	Chemical Formula
COMPMM1(S)	NH ₃ ·MMG(S)
COMPMM2(S)	Ga·NH ₂ ·MMG(S)
COMPMM3(S)	NH ₃ ·Ga·NH ₂ ·MMG(S)
COMPMM4(S)	Ga·NH ₂ ·Ga·NH ₂ ·MMG(S)
COMPMM5(S)	NH ₃ ·Ga·NH ₂ ·Ga·NH ₂ ·MMG(S)
RINGM1(S)	NH ₂ ·Ga·NH ₂ ·Ga·NH ₂ ·Ga(S)
RINGM2(S)	(S)NH ₂ ·Ga·NH ₂ ·Ga·NH ₂ ·Ga(S)
COMPMM1(S)	MMG·GaNH ₂ (S)
COMPMM2(S)	NH ₃ ·MMG·GaNH ₂ ·Ga(S)
COMPMM3(S)	NH ₂ ·Ga·NH ₂ ·Ga(S)
COMPMM4(S)	MMG·NH ₂ ·Ga·NH ₂ ·Ga(S)
COMPMM5(S)	NH ₃ ·MMG·NH ₂ ·Ga·NH ₂ ·Ga(S)
TCOM1(S)	NH ₃ ·TMG(S)
TCOM2(S)	NH ₂ ·DMG(S)
TCOM3(3)	(S)NH ₂ ·DMG(S)
COM1(S)	RINGM2(S)-CH ₃ complex



OUTPUT Results



1. Lattice Constant :

- Layer by layer lattice constant Extraction.
- Averaging layer by layer lattice constant may produce overall lattice constant of film.
- The lattice constant can be calibrated with XRD studies obtained lattice constant .
- Lattice constant includes all the strain, defects etc effects.

2. Strain:

- Averaging layer by layer strain will produce overall strain in the film.
- The strain can be calibrated with experimental strain.

3. Surface Roughness:

- User may extract surface roughness w.r.t time, included through

$$r = \sqrt{\frac{\sum_{i=1}^N \sum_{j=1}^N [h_{ij} - \bar{h}]^2}{N \times N}}$$

Here N is the total number of lattice points, h_{ij} is the height at a given lattice point located at position i and j , on the lattice and \bar{h}_{avg} is the average height of all lattice points.

4. Mole fraction:

- User may extract number of atoms of different constituents layer by layer.
- Ratio of group-III & V atoms, molefraction can be produced.

5. Defects :

- User may extract number of interstitials, vacancy etc layer by layer



Case Study Results



Controlled Epitaxial Growth of GaAs in real MOCVD Reactor Environment*

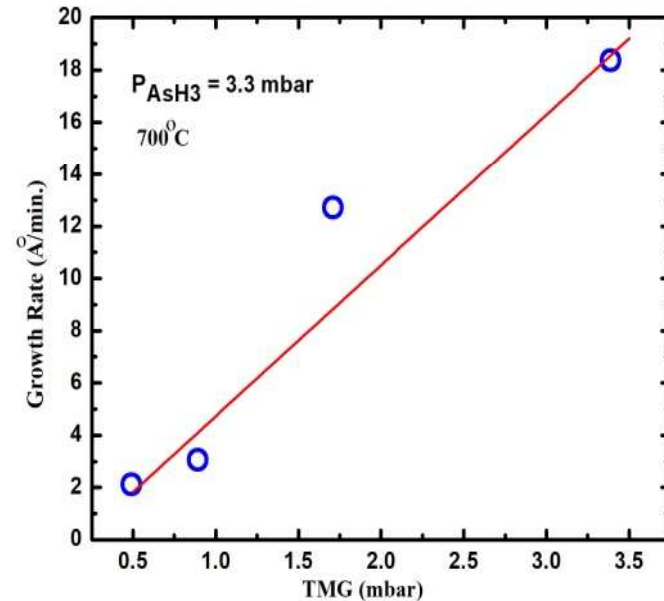
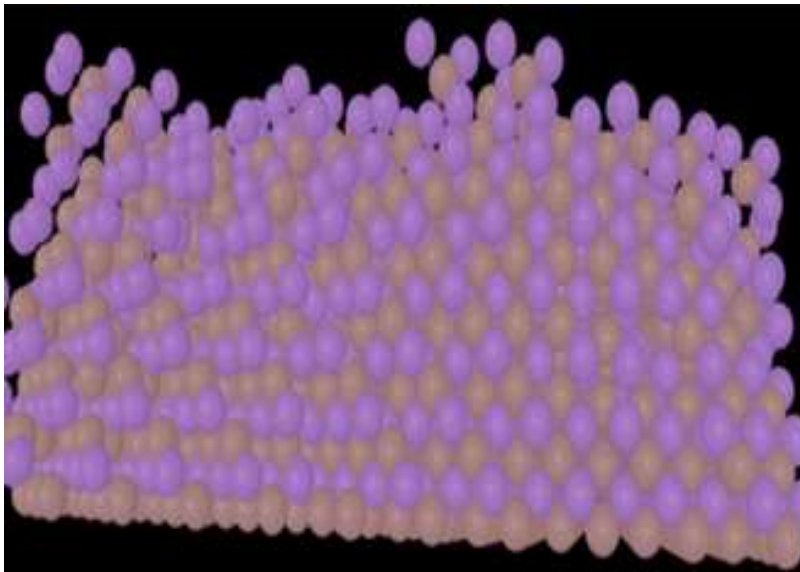
*P. K. Saxena, P. Srivastava, R. Trigunayat, An innovative approach for controlled epitaxial growth of GaAs in real MOCVD reactor environment, [*Journal of Alloys and Compounds* 809 \(2019\) 151752.](#)



GaAs: MOCVD EpiGrowth



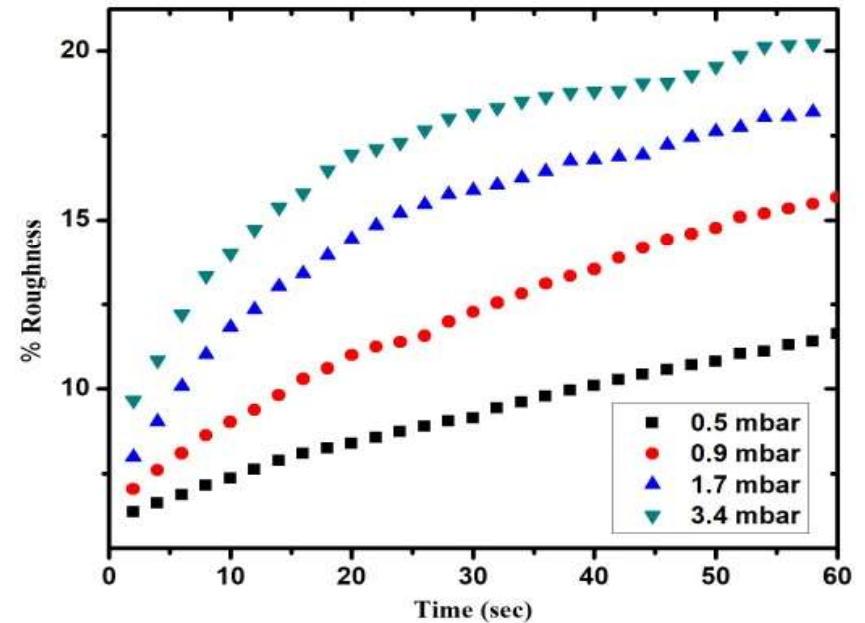
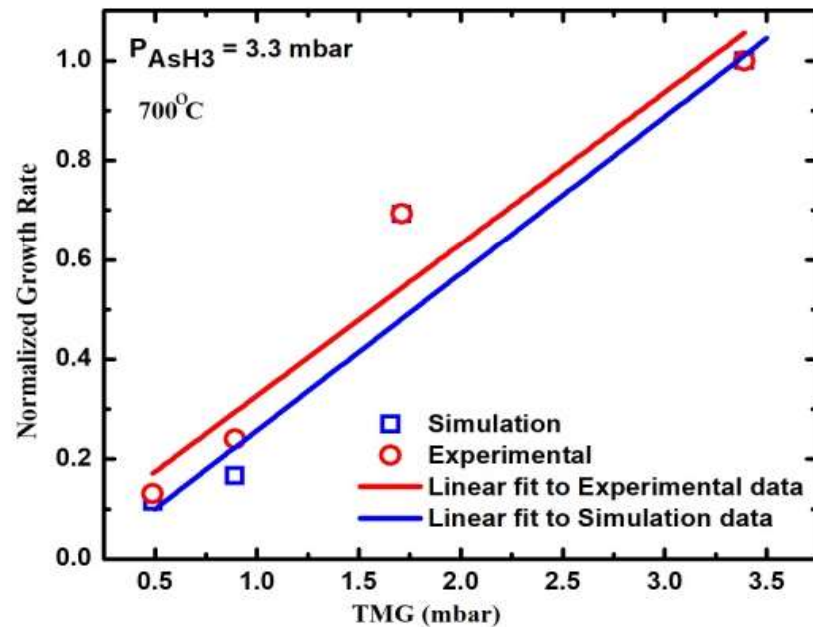
GaAs monolayers growth over GaAs



* [Journal of Alloys and Compounds 809 \(2019\) 151752.](#)



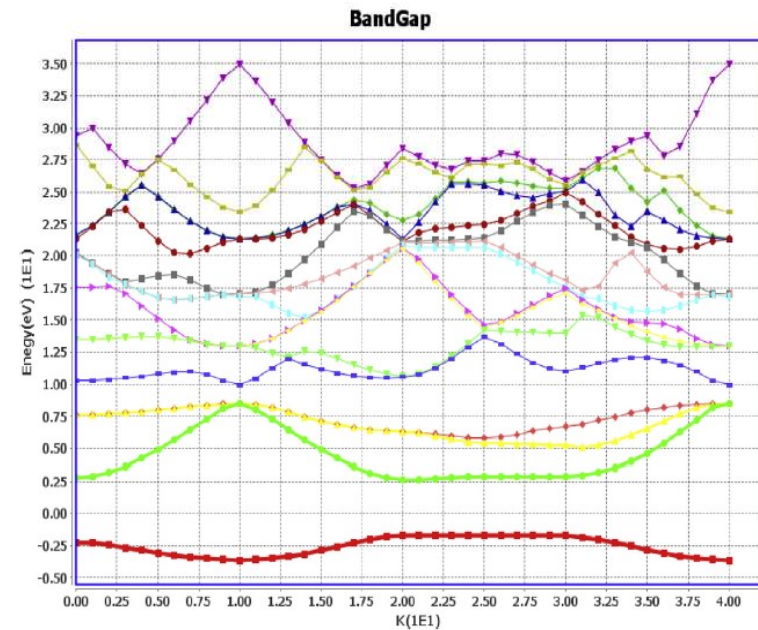
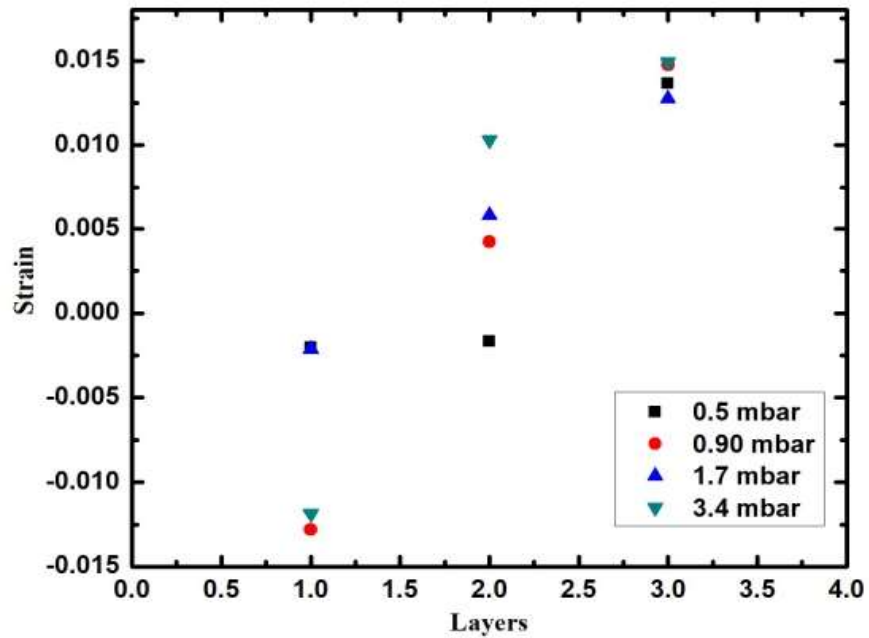
GaAs: MOCVD EpiGrowth



* [Journal of Alloys and Compounds 809 \(2019\) 151752.](#)



GaAs: MOCVD EpiGrowth



* [Journal of Alloys and Compounds 809 \(2019\) 151752.](#)





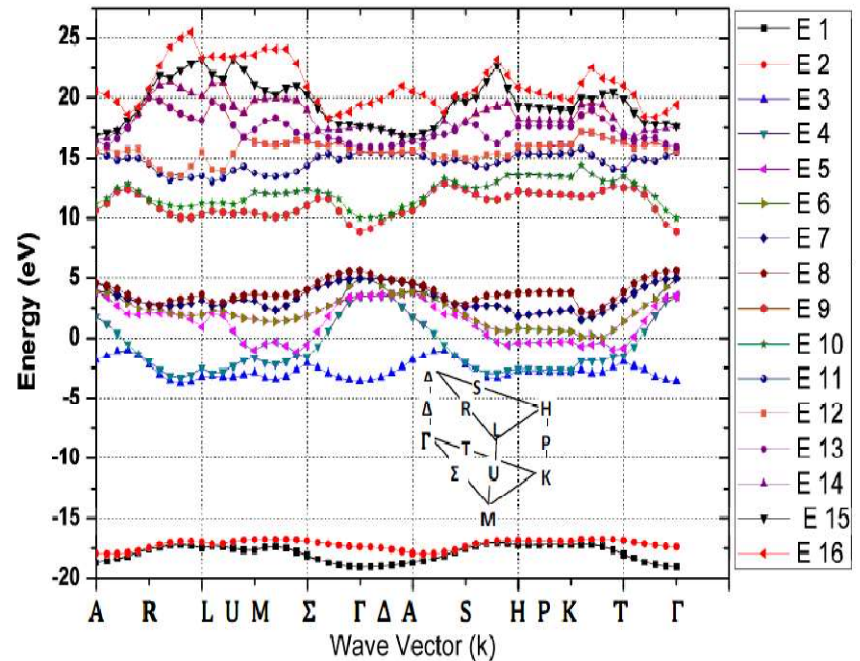
Material Characterization of thin/thick Film



Full Band Structure



- ❑ Electronic band structure of IV, III-V and II-VI alloys using standard lattice constant “a”
- ❑ Virtual Crystal Approximation for ternary alloys.
- ❑ Semi-empirical disorder contribution.
- ❑ Non-Parabolicity & Parabolicity effects
- ❑ Main valleys energies, effective masses with non-parabolicity factors, carrier group velocity, DOS etc.



Case Studies- Results



Material Characterization through Electronic Transport on Band Structure

* Praveen K Saxena *at. el.*, [An Innovative Model for Electronic Band Structure Analysis of doped and undoped ZnO](#), *Journal of Electronic Materials* Under Review, 2020.

*Anshika Srivastava, Anshu Saxena, Praveen K. Saxena, F. K.Gupta, Priyanka Shakya, *at. el.*, [An innovative technique for electronic transport model of group-III nitrides](#), *Scientific Reports nature research* (2020) 10:18706.



ZnO: Full Band Simulator



Different DFT based calculated energy band gap of ZnO materials within the conventional DFT (LDA and PBE functional), LDA + U functional, and hybrid functional (HSE06) along with the lattice parameters, structural internal parameters (u) and disorder constants (P).

DFT Methods	LDA	PBE	HSE06	LDA+U	Experimental	This Work
a (Å)	3.210 ³	3.284 ^{4.5}	3.262 ^{4.5}	3.197 ⁶	3.253 ¹⁹⁻²¹	3.254
c (Å)	5.136 ³	5.296 ^{4.5}	5.212 ^{4.5}	5.154 ⁶	5.205 ¹⁹⁻²¹	5.21
u	0.380	0.378	0.381	0.378	0.380	0.380
P*	0.000	0.002	-0.001	0.002	0.000	0.000
Eg (eV)	0.7941³	3.413^{4.5}	2.464^{4.5}	1.1541⁶	3.44³⁻⁵	3.428

* [Journal of Electronic Materials \(under Review\).](#)



ZnO: Full Band Simulator



ZnO Samples	t_{DS} (nm)			t_{WH} (nm)	Strain	Lattice Constant		Internal Parameter u(P)	Bond Length (Å)	Optical Band gap (eV)	Simulated Band gap (eV)
	(100)	(002)	(101)			a (Å)	c (Å)				
Undoped	11	18	10	26	6.5×10^{-3}	3.246	5.238	0.398	2.013	3.22	3.22
0.45at.% Cd	16	20	17	13	-8.0×10^{-3}	3.328	5.190	0.4023	2.009	3.20	3.19
0.51at.% Cd	19	21	19	26	1.5×10^{-3}	3.332	5.161	0.4025	2.007	3.19	3.22
0.56at.% Cd	11	18	10	31	10.0×10^{-3}	3.313	5.225	0.4040	2.006	3.15	3.15
1at.% Sr	14	10	17	7.48	-1.64×10^{-2}	3.256	5.194	0.389	1.978	3.25	3.27
2at.% Sr	21	9	16	10.27	4.27×10^{-2}	3.251	5.194	0.389	1.976	3.26	3.26
3at.% Sr	9	6	6	4.14	9.95×10^{-2}	3.271	5.223	0.389	1.988	3.28	3.33
1at.% Fe	5	8	9	1.43	-14.8×10^{-2}	3.236	5.194	0.380	1.967	3.24	3.26
2at.% Fe	3	5	7	0.65	-34.5×10^{-2}	3.231	5.194	0.380	1.968	3.26	3.25
3at.% Fe	8	5	7	9.06	6.6×10^{-2}	3.231	5.186	0.380	1.970	3.29	3.25

Undoped, Cd, Sr and Fe doped ZnO thin films (Sol gel) along with optical and simulated energy band gaps

* [Journal of Electronic Materials \(under Review\).](#)



Group-III Nitrides: Full Band Simulator



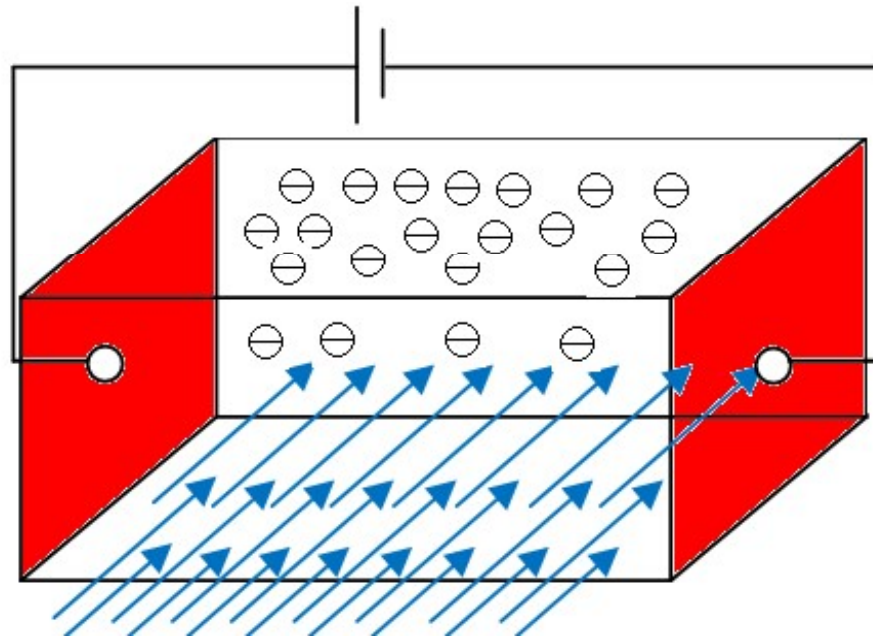
Energy difference obtained using FullBand simulator compared with various density functional theory (DFT) techniques and with experimental results

Material	Previously reported values of E_g	E^{LDA}	$E^{LDA-1/2}$	DFT^{PBE}	DFT^{HSE}	Experiments	$E^{This\ work}$
AlN	6.54 ⁷ , 6.23 ¹⁰	4.50 ^{5,7}	6.06 ⁵	4.13 ⁷ , 4.02 ²⁰	6.42 ⁷ , 6.29 ²⁰	6.23 ⁵ , 6.026 ¹⁷ , 6.1-6.27 ²⁰	6.20
GaN	3.5 ⁷ , 3.507 ¹⁰	2.02 ⁵ , 2.11 ⁷	3.52 ⁵	1.69 ^{7,20}	3.55 ⁷ , 3.55 ²⁰	3.507 ⁵ , 3.35 ²² , 3.51 ²⁰	3.47
InN	0.7-1.0 ^{7,8} , 0.7-1.9 ¹⁰	-0.03 ⁵ , -0.24 ⁷	0.95 ⁵	-0.42 ^{7,20}	0.86 ⁷ , 0.86 ²⁰	0.7-1.9 ⁵ , 0.6-0.7 ²⁰	0.7
Al _{0.2} Ga _{0.8} N	3.99*	2.353 ⁵	3.951 ⁵	4.570 ¹²	4.569 ¹²	3.962 ²⁴	3.94
In _{0.2} Ga _{0.8} N	2.72-2.78*	1.52 ⁵	2.76 ⁵	2.272 ⁵	1.925 ¹²	2.625 ²³	2.66
In _{0.2} Al _{0.8} N	4.7 - 4.76*	3.431 ⁵	4.409 ⁵	3.445 ¹²	2.976 ¹²	4.515 ²⁵	4.71

* Scientific Reports, Nature Journal .



MOBILITY CHARACTERIZATION



MATERIAL CHARACTERIZATION



Free Electrons

- For free particles, the electron wave function is the solution to the time-independent Schrödinger equation:

$$\left(\frac{\hbar^2}{2m} \nabla^2 + E \right) \phi(r) = 0$$

- The solutions form the basis of plane waves:

$$\phi_{\mathbf{k}}(r) = C_{\mathbf{k}} e^{i\mathbf{k} \cdot r} \quad \text{with} \quad k^2 = k_x^2 + k_y^2 + k_z^2 = \frac{2mE}{\hbar^2}$$

- The velocity, \mathbf{v} , of a particle represented by a wave packet centered around the crystal momentum, \mathbf{k} , is obtained from the dispersion relation between \mathbf{k} and the energy E as

$$E_{\mathbf{k}} = \frac{\hbar^2 k^2}{2m} \dots \dots \dots \mathbf{v} = \left\langle \left| \frac{\hbar}{i} \nabla \right| \right\rangle = \frac{1}{\hbar} \nabla_{\mathbf{k}} E_{\mathbf{k}} = \frac{\hbar \mathbf{k}}{m} \quad \text{and} \quad D(E) dE = \frac{2m^{3/2} E^{1/2}}{\sqrt{2\pi^2 \hbar^3}} dE$$



ELECMOB SIMULATOR



- The Boltzmann Transport Equation (BTE) is

$$\frac{df}{dt} + \nabla_k E(k) \cdot \nabla_r f + F \cdot \nabla_p f = \left. \frac{df}{dt} \right|_{\text{scattering}} + GR$$

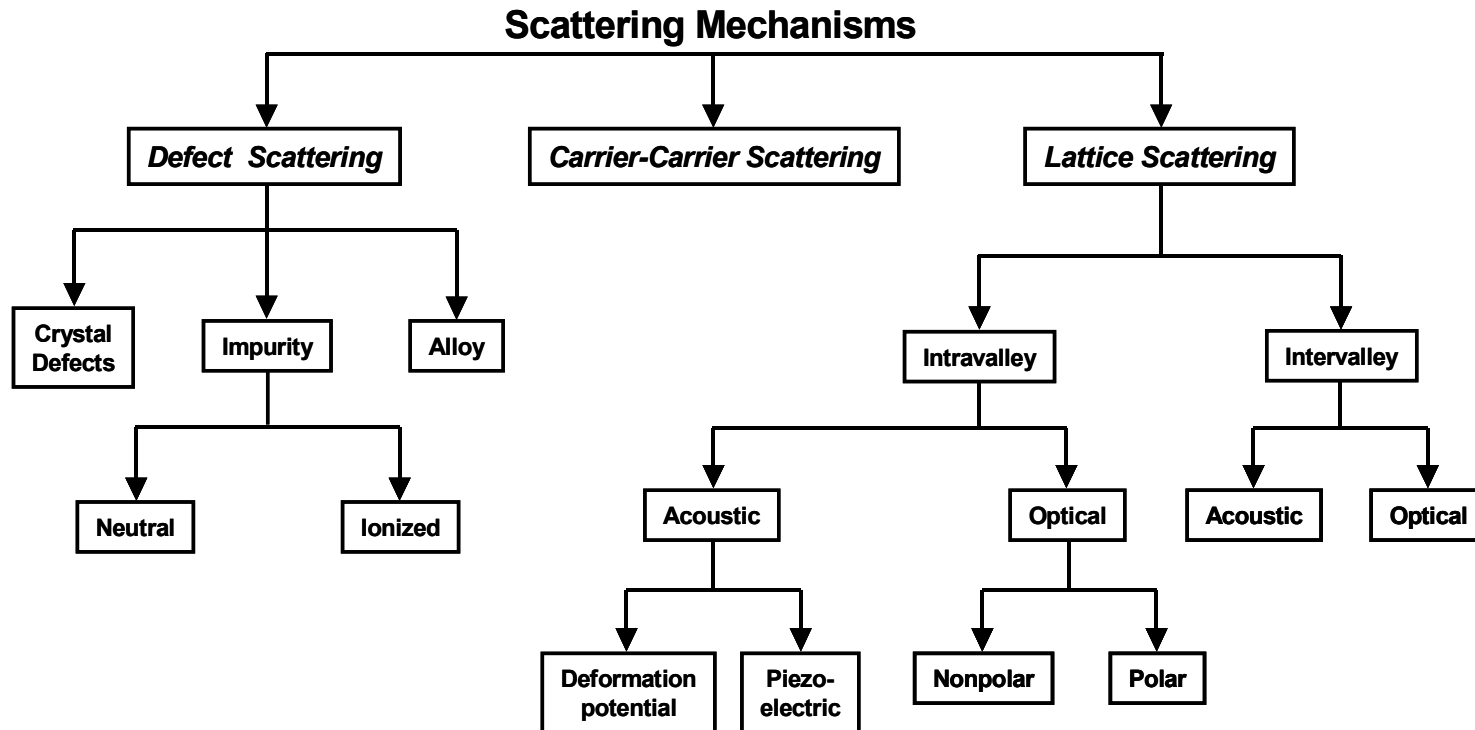
Here f is the distribution function, E is the electric field, F is the external electromagnetic force.

- Solution of 6+1 dimensional is possible through:

- A spherical harmonic expansion (SHE) method with initial approximations
 - accuracy of simulation results ??
- The ensemble Monte Carlo (EMC) technique (stochastic) is best suited to simulate non-equilibrium transport in semiconductor.
- In Monte Carlo (MC) method, physics is more straightforward and provides flexibility in exploring physical mechanisms and carrier transport.



SCATTERING MECHANISMS



ELECMOB SIMULATOR



Under the influence of Electromagnetic forces the carrier:

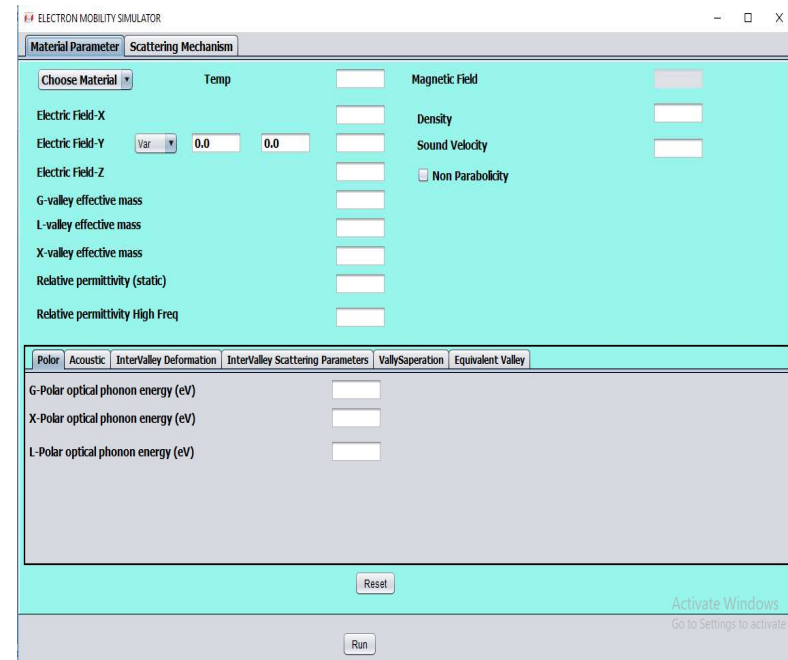
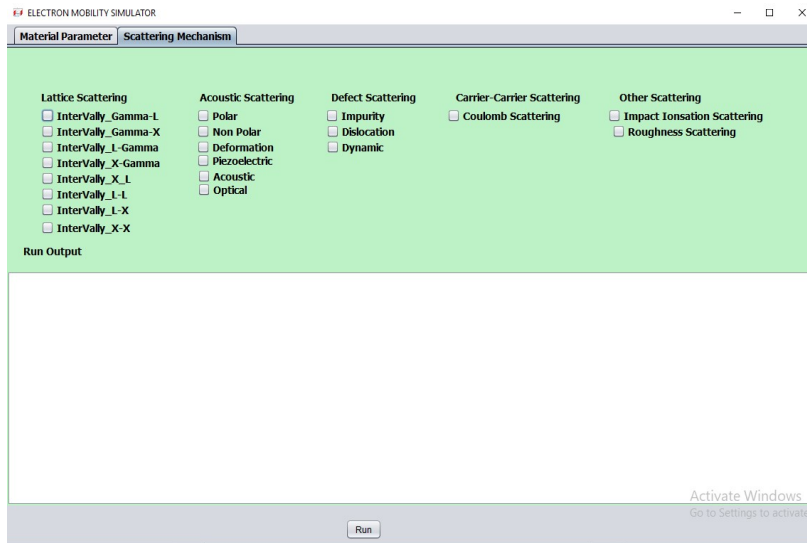
$$k(t) = k(v) - \frac{e(E + v \times B)t}{\hbar}$$

where

$$v = \frac{1}{\hbar} \frac{dE}{dk}$$

&

$$\frac{\partial k}{\partial t} = \frac{qE}{\hbar}$$

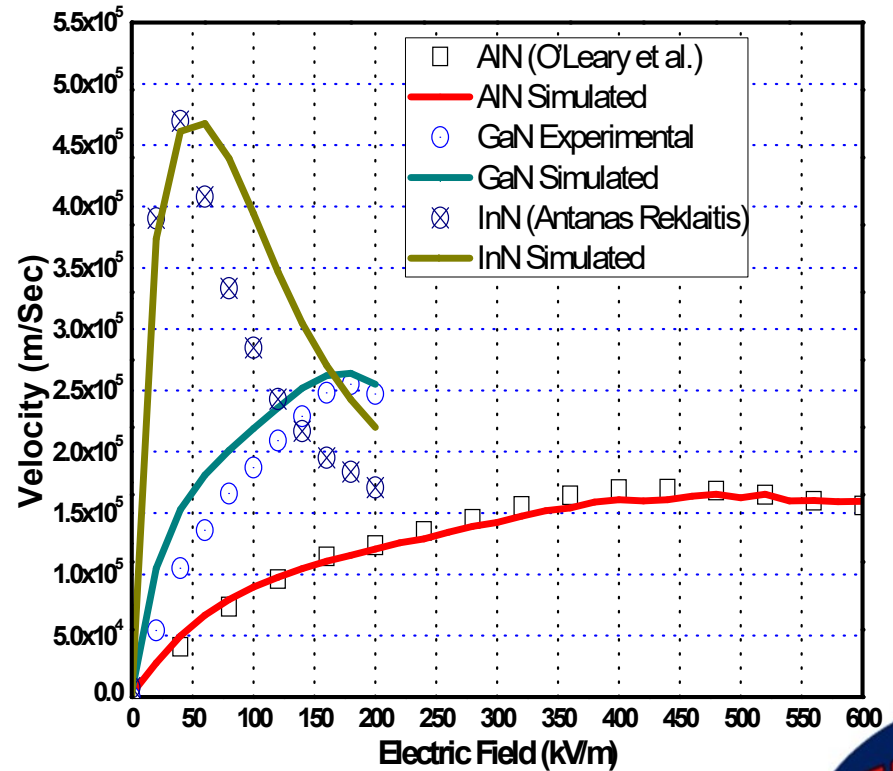


GROUP-III NITRIDES

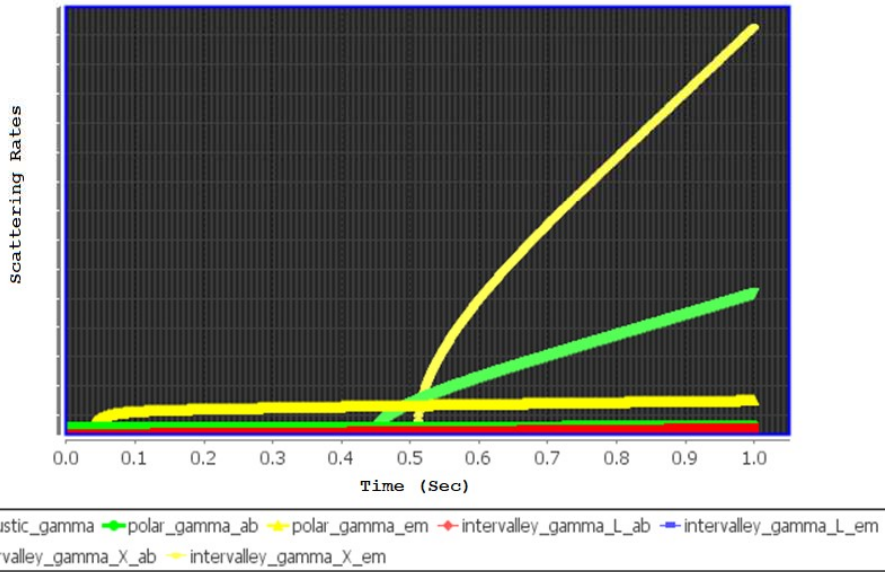


The Comparison of simulated electron drift velocity as a function of applied electric field with the reported literature. Data from present work is displayed as solid lines where as experimental/theoretical results are depicted by open circles, squares and triangles for AlN, GaN and InN respectively.

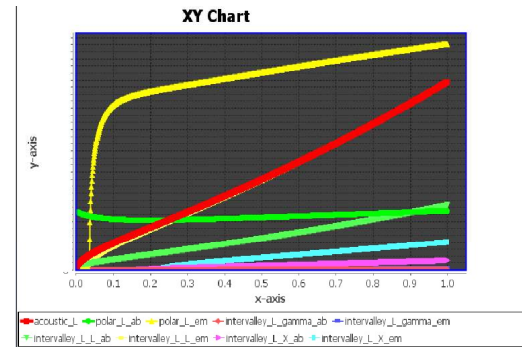
❖ Anshika Srivastava, Anshu Saxena, Praveen K. Saxena, F. K. Gupta, Priyanka Shakya, *at. el.*, An innovative technique for electronic transport model of group-III nitrides, [Scientific Reports nature research](#) (2020) 10:18706.



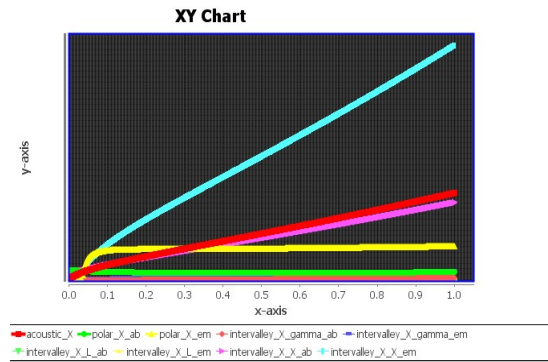
SCATTERING RATES



F- Valley



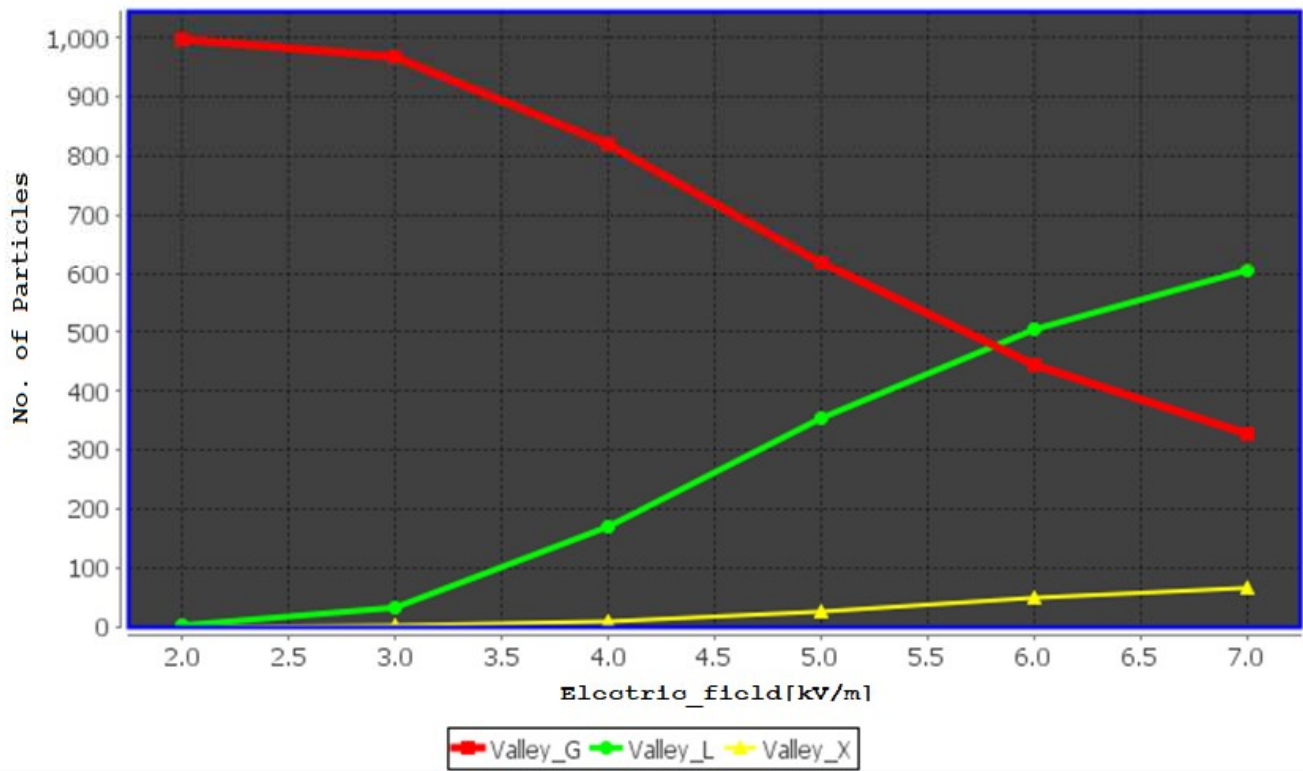
U- Valley



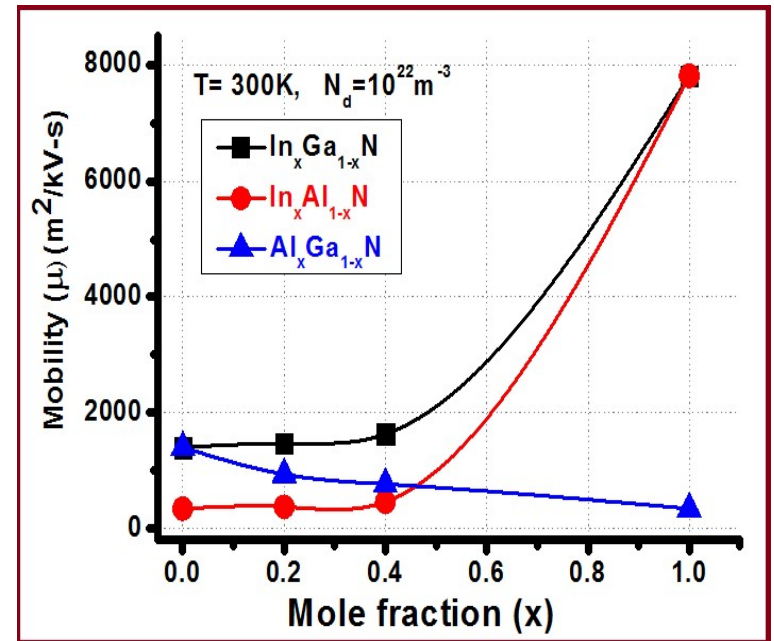
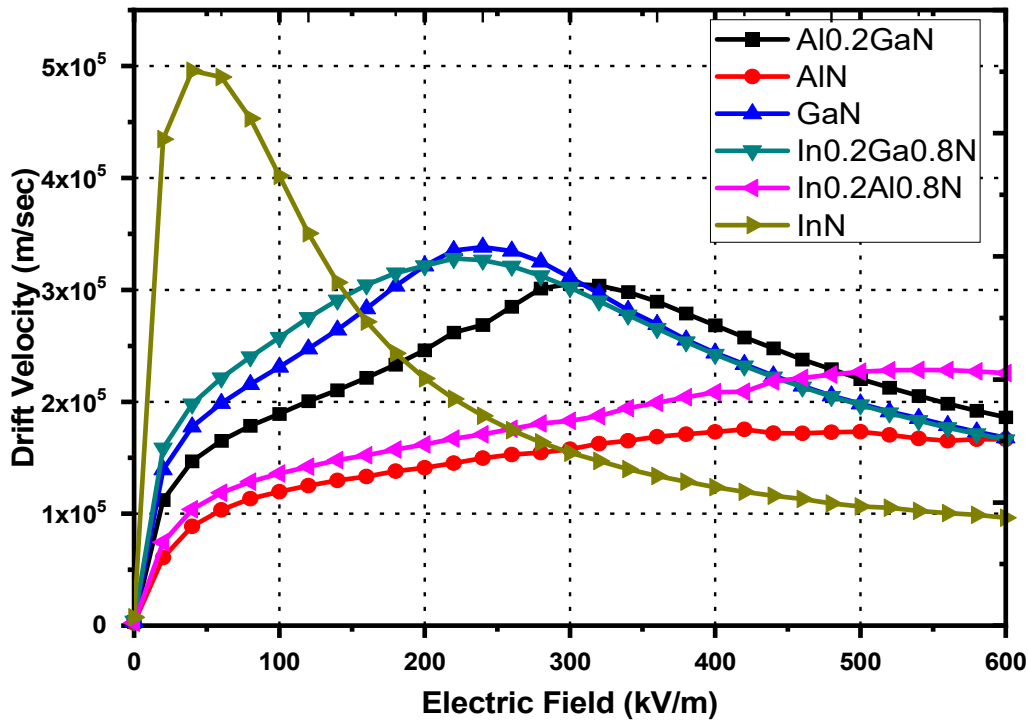
Γ_3 - Valley



OCCUPATION



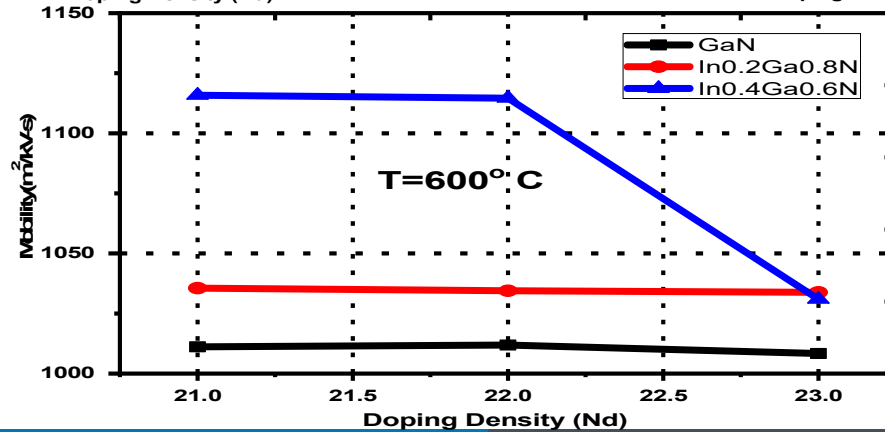
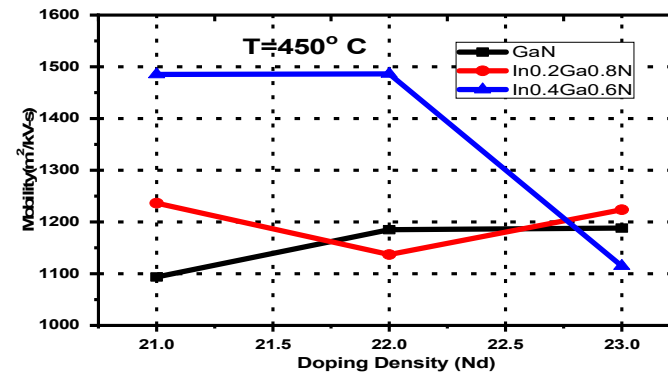
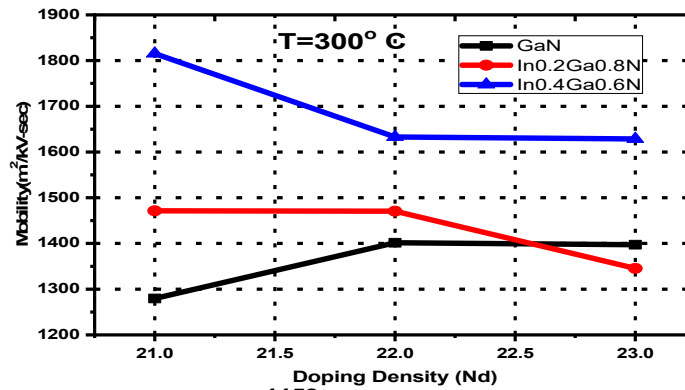
MOBILITIES



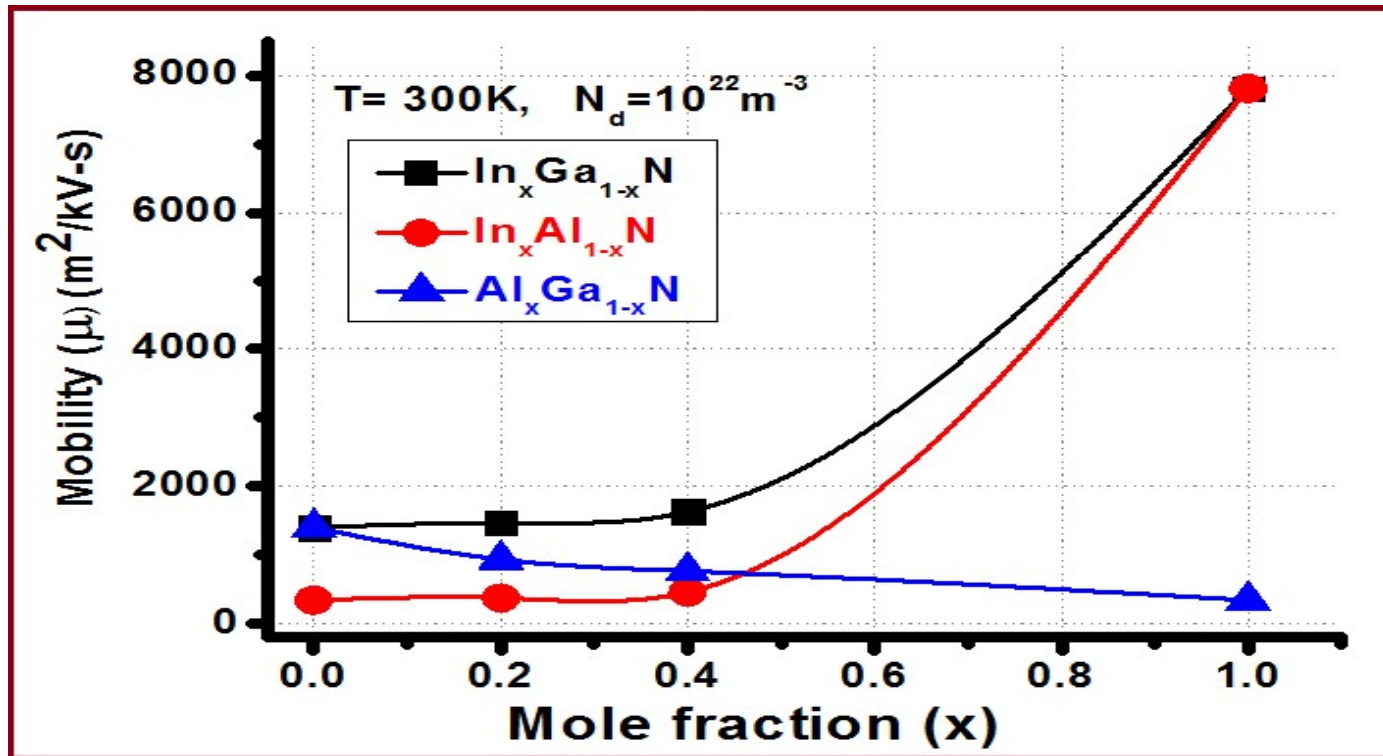
* Scientific Reports, Nature Journal.

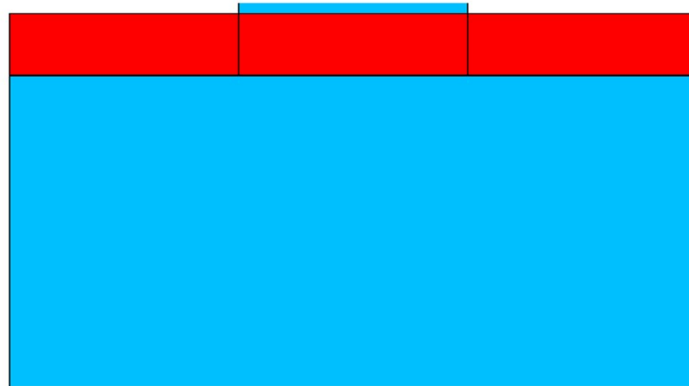


TEMP EFFECT ON MOBILITIES



MOBILITIES TERNARY COMPOUNDS

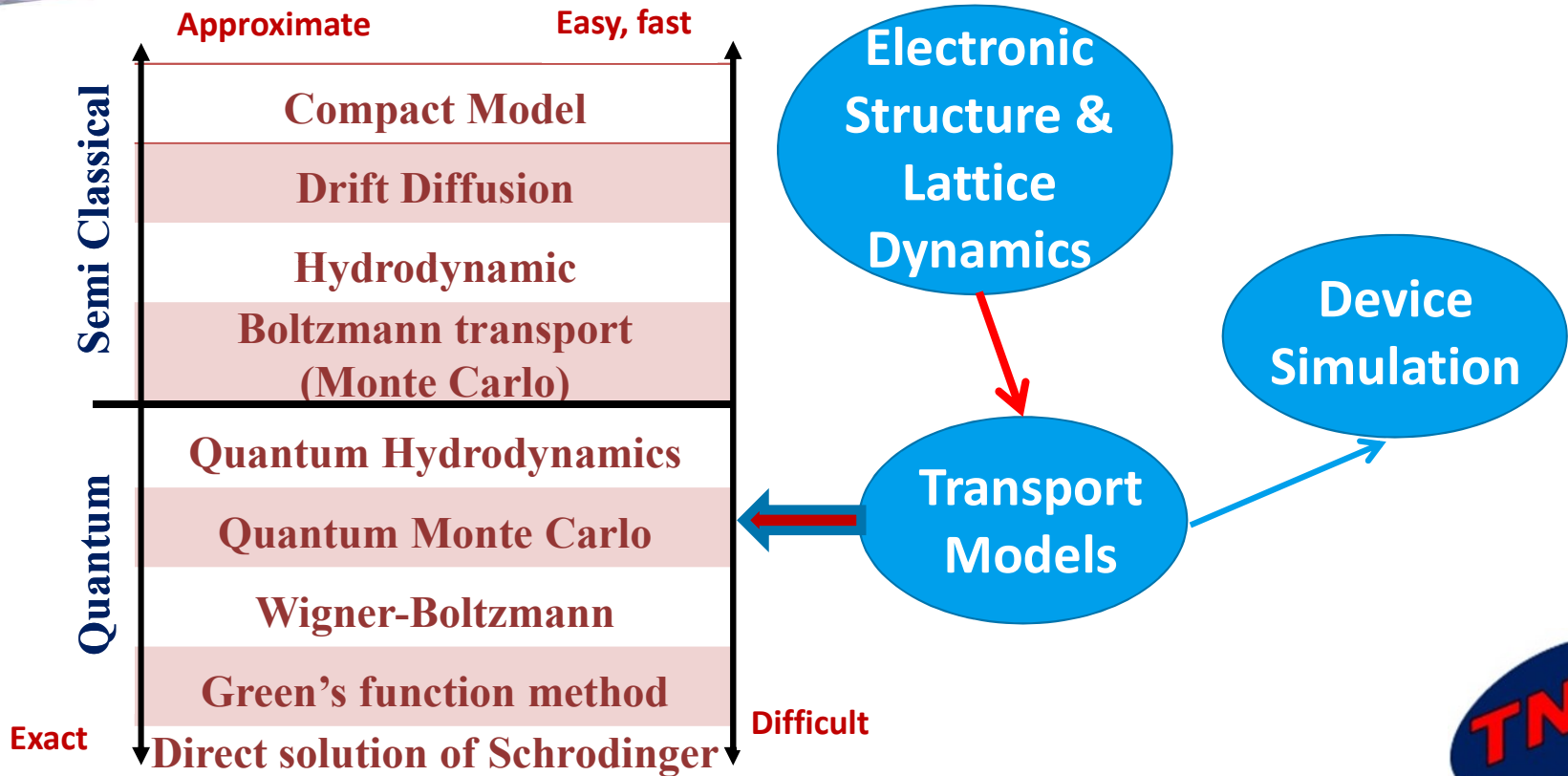




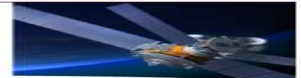
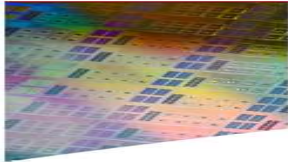
*Technology of Next Level
driven through innovation*

Monte Carlo Particle Device Simulator

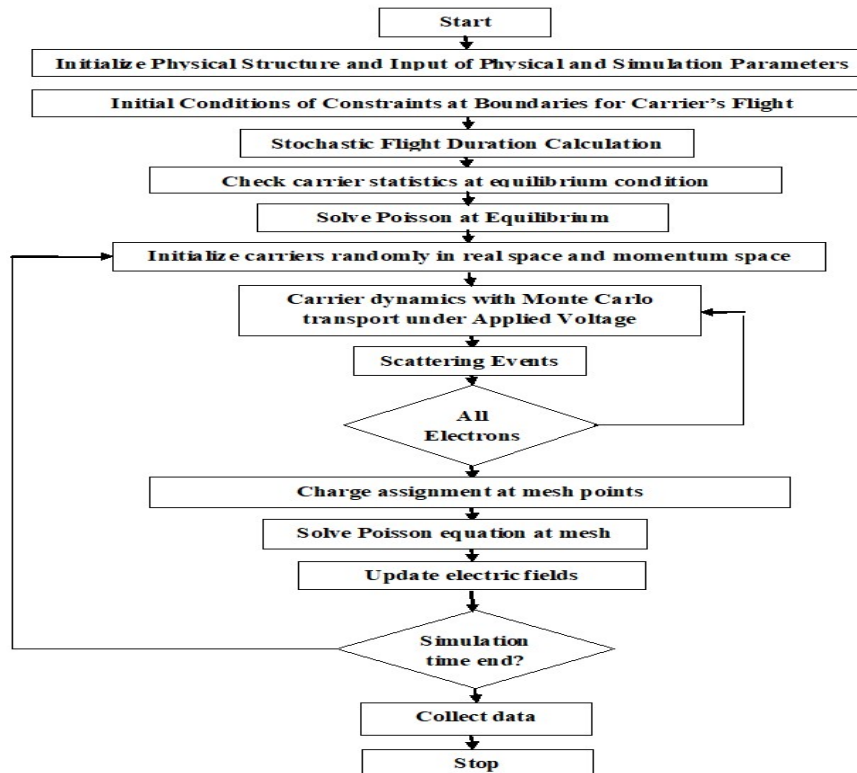
DEVICE MODELING



FLOW CHART



Flow Chart for program implementation



Case Studies



GaN FET Simulation

*P. K. Saxena *et. al.*, Atomistic Level Process to Device Simulation of GaNFET Using TNL TCAD Tools, [Book Chapter](#), © [Springer Nature](#) (2020) 176, Lecture Notes in Electrical Engineering ISBN 978-981-15-5261-8 ISBN 978-981-15-5262-5 (eBook)



GaNFET Epitaxial Growth

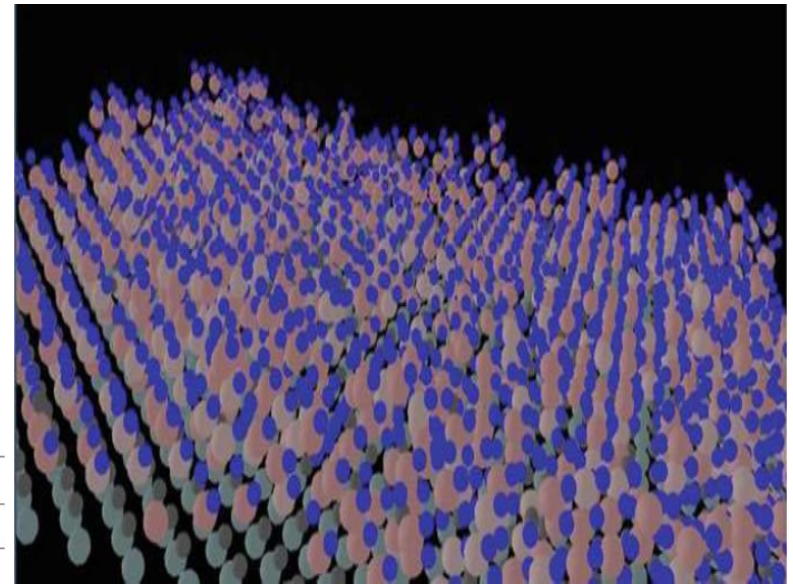


Epi-growth has been done with the following process parameters:

Parameters	Values	Unit
Time	30	s
Temperature	800	°C
Surface energy	2	eV
Desorption barrier energy	4	eV
Schwoebel barrier	0.002	eV
Incorporation barrier	0.05	eV
Nearest neighbor attraction	0.05	eV

Precursors and gas ambience used during simulation

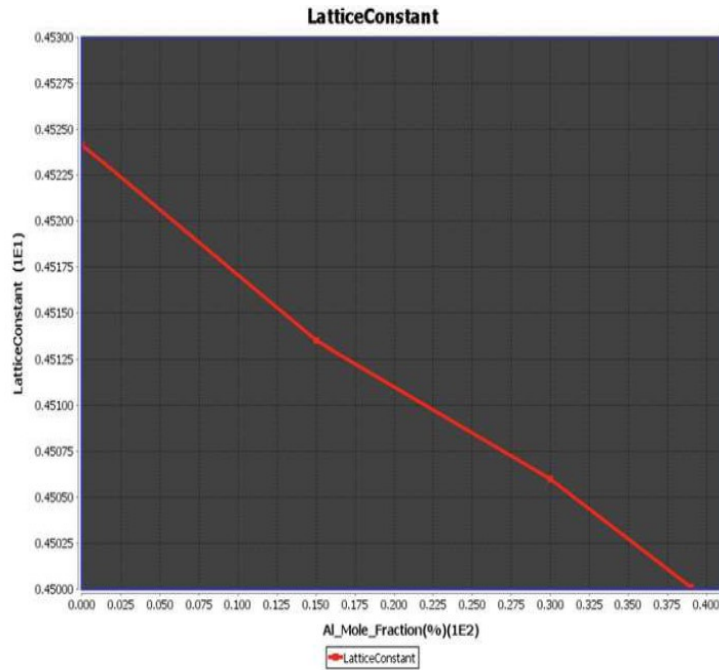
Materials	Partial pressure		
	Ga (mbar)	Al (mbar)	N ₂ (mbar)
GaN	0.3	0.0	3.0
Ga _{0.85} Al _{0.15} N	0.3	0.03	3.0
Ga _{0.7} Al _{0.3} N	0.28	0.05	3.0
Ga _{0.61} Al _{0.39} N	0.25	0.10	3.0



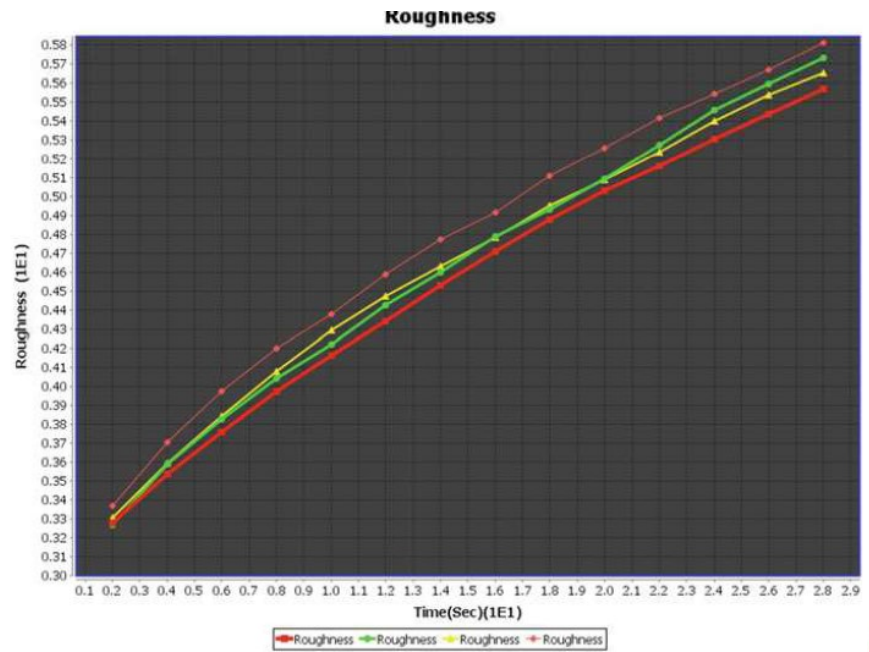
GaNFET Case Studies



Variation of lattice constant with Al mole fraction



Surface roughness at the interface of AlGaN/GaN



GaNFET Case Studies

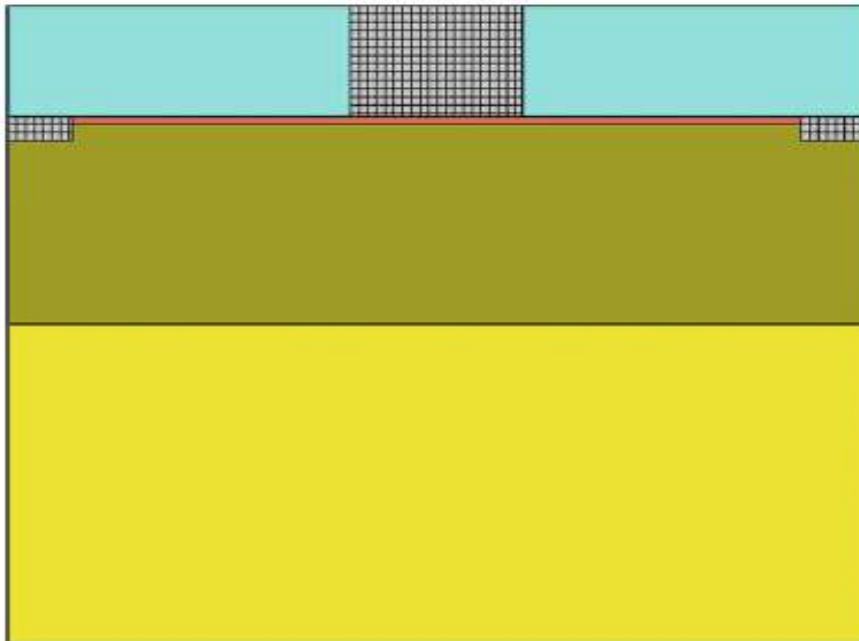
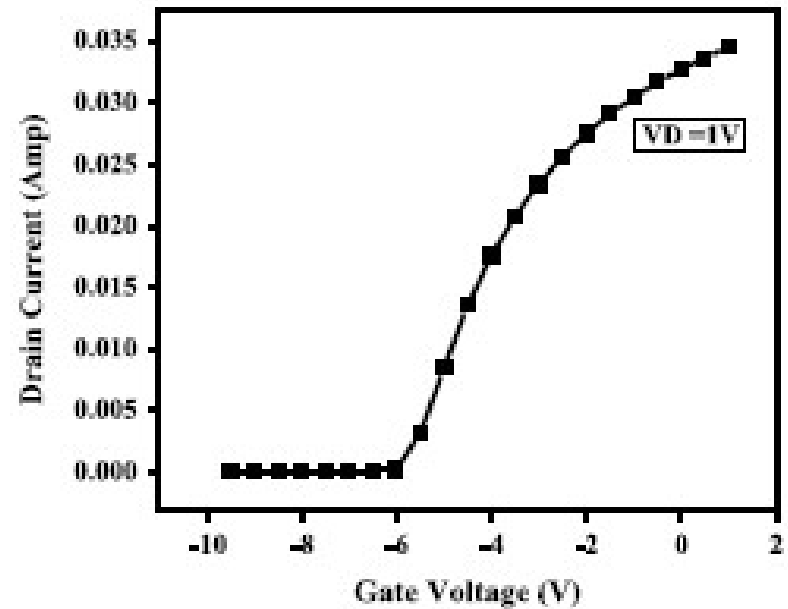
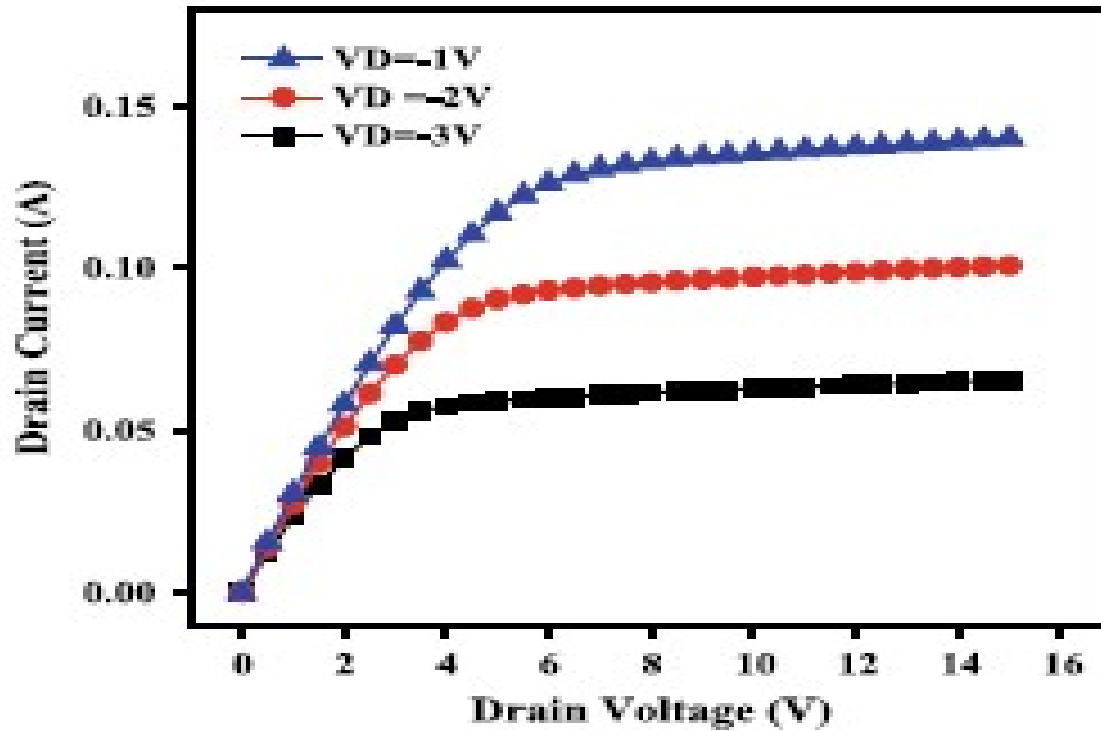


Fig. 9 Device structure with 25 nm thick AlGaN/GaN layer grown on SiC (100) substrate



GaNFET Case Studies



Optical Device



InGaAs/InP Infrared Photodetector

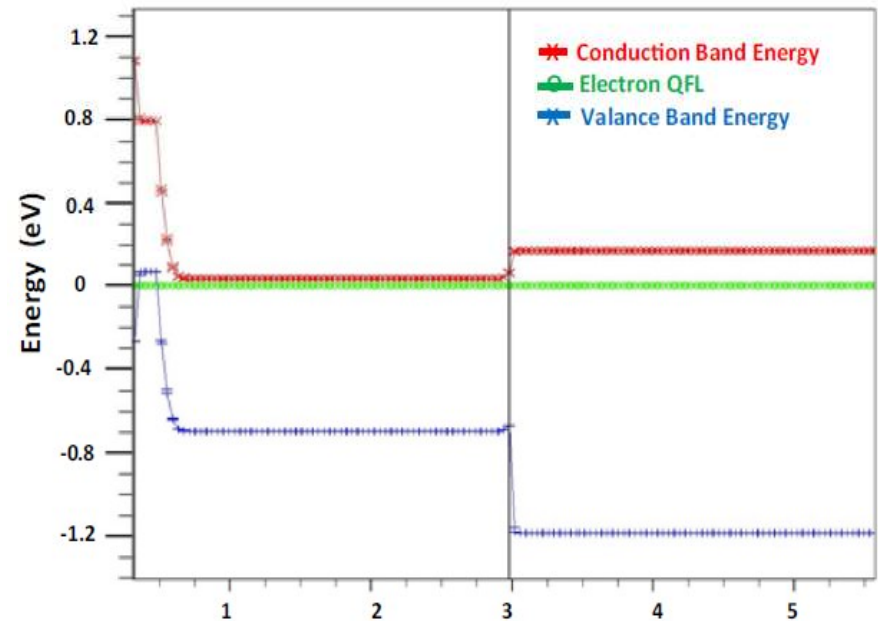
*P. K. Saxena *at. el.*, Numerical simulation of $\text{In}_x\text{Ga}_{1-x}\text{As}/\text{InP}$ PIN photodetector for optimum performance at 298 K, [*Optical and Quantum Electronics*](#) (2020) 52:374



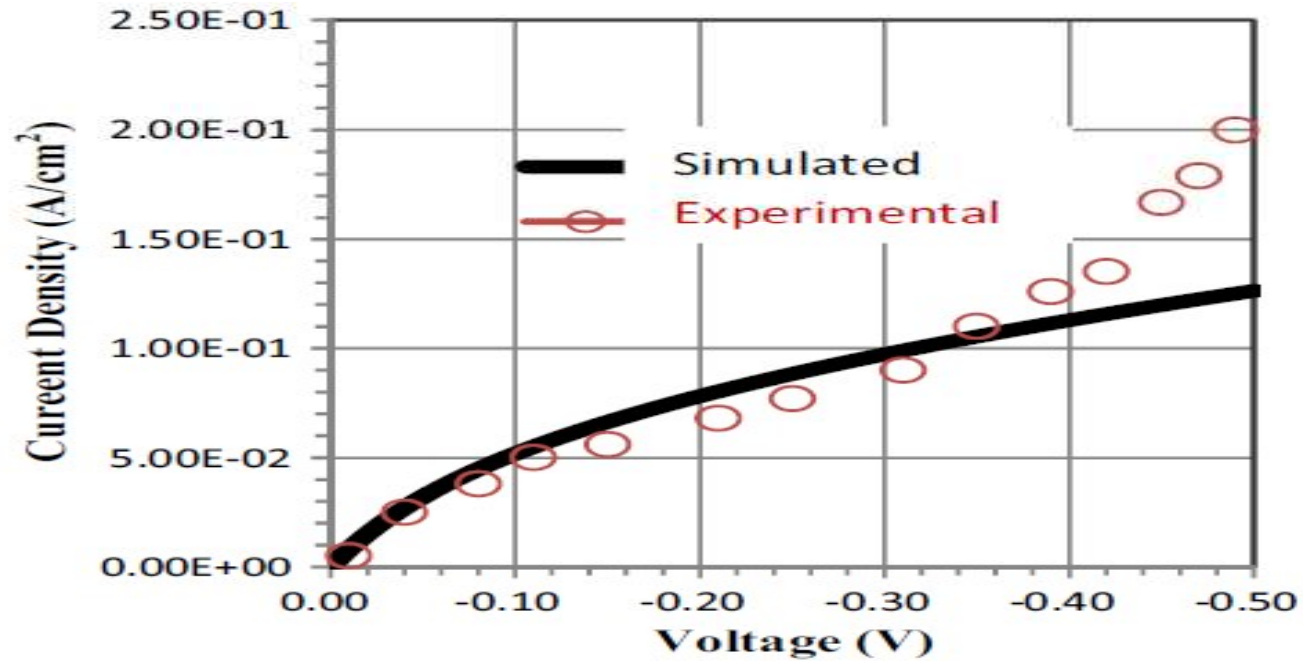
Infrared Detector



p^+ $\text{In}_{0.53}\text{Ga}_{0.47}\text{As}$ (150 nm)	p - InP	i - $\text{In}_{0.53}\text{Ga}_{0.47}\text{As}$ (2.5 μm)	n -InP (2.6 μm)
--	--------------	--	----------------------------------



I – V Characteristics

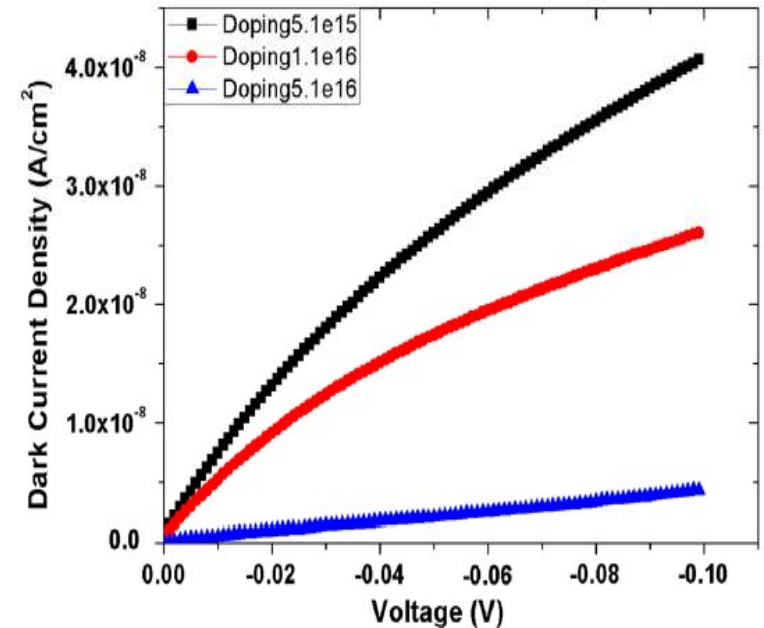


Infrared Detector

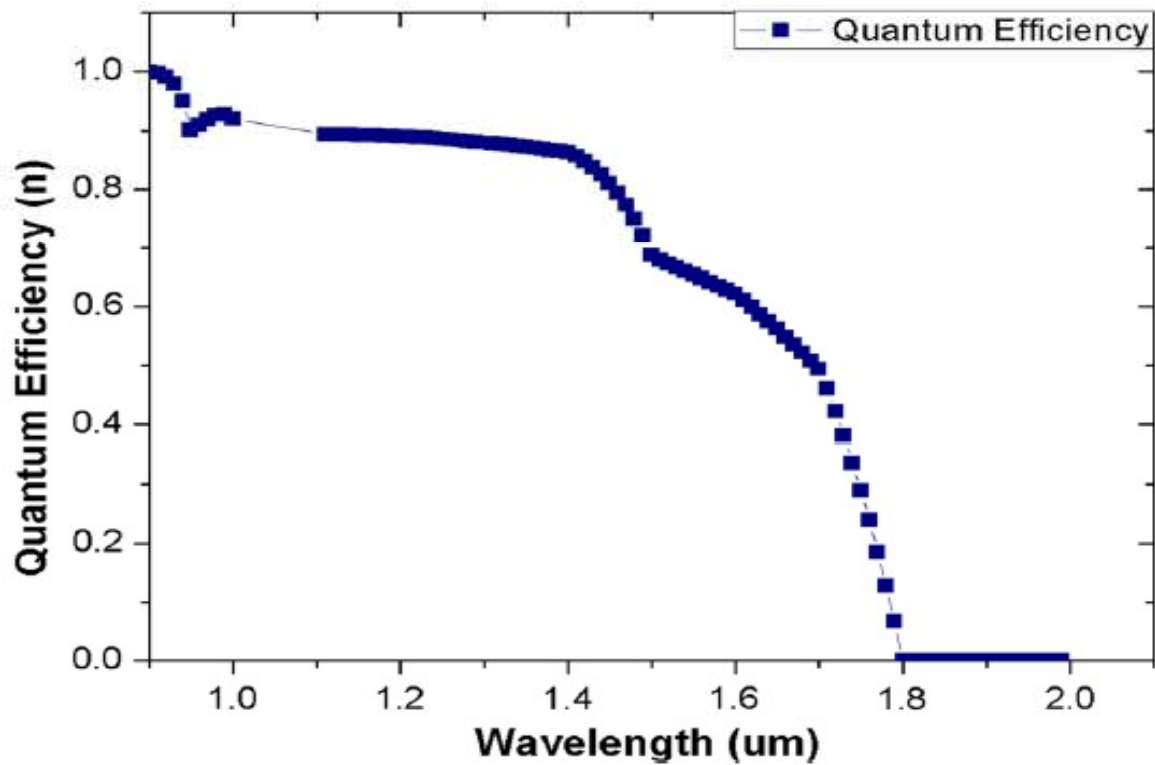


Table 1 The current density values for different doping dose at specified absorbing layer thickness

Doping dose (cm^{-3})	Current density at specified absorbing layer thickness (A/cm^2)		
	2 μm	2.5 μm	3 μm
5.1×10^{15}	2.53×10^{-07}	2.53926×10^{-07}	2.54×10^{-07}
1.1×10^{16}	1.62×10^{-07}	1.63×10^{-07}	1.63×10^{-07}
5.1×10^{16}	2.6456×10^{-08}	2.6898×10^{-08}	2.7595×10^{-08}



Quantum Efficiency



FDSOI MOSFET

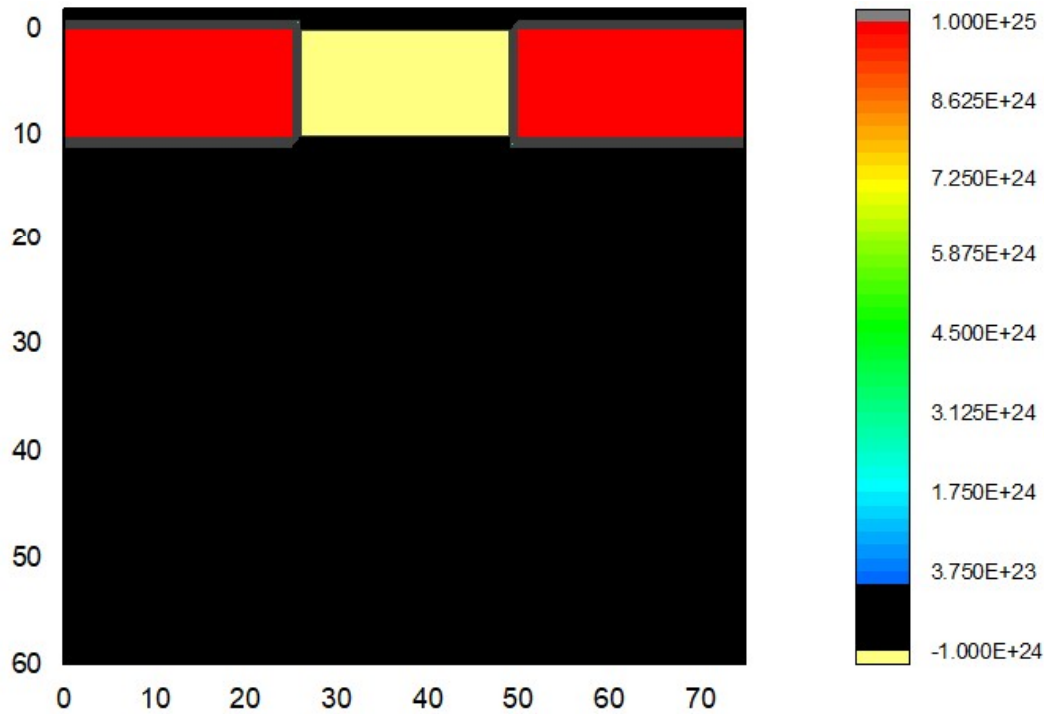


FDSOI MOSFET

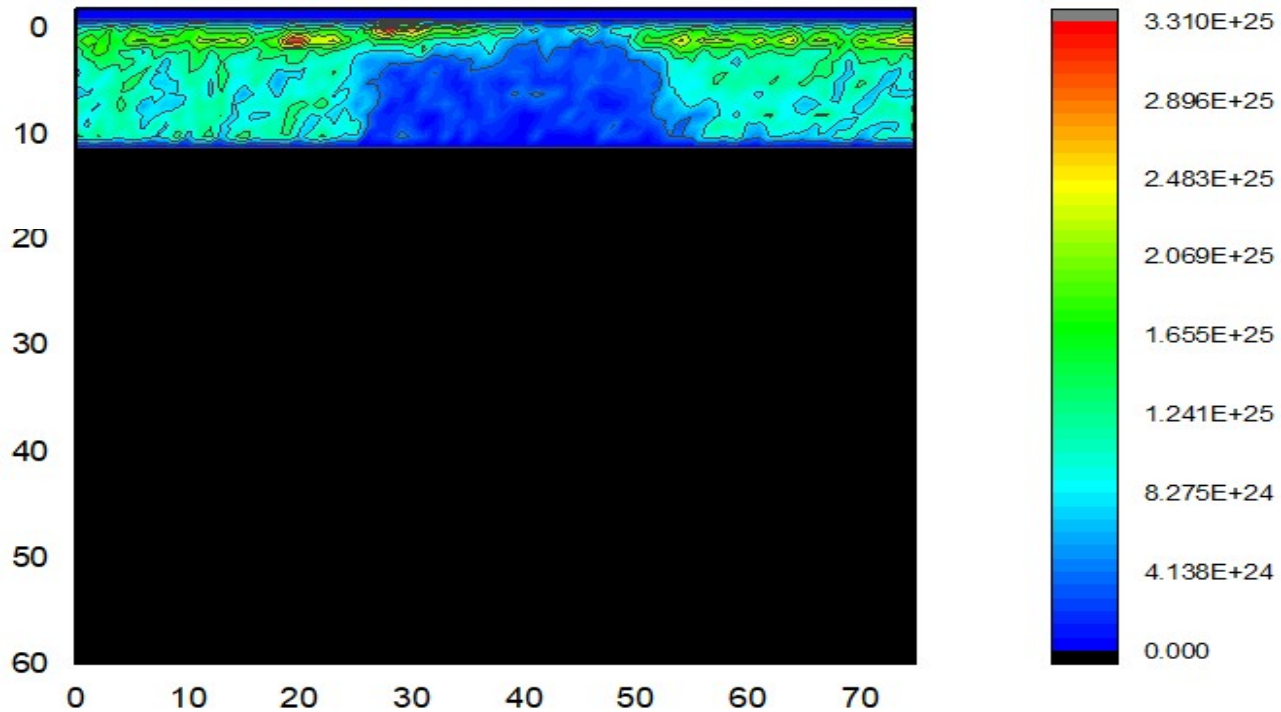
*P. K. Saxena *et. al.*, A Comparative Study for Scaling FDSOI Technology up to 7nm –Based on Particle device Simulation, *Journal of Nano & Optoelectronics*(2020), under Review.



FDSOI MOSFET



FDSOI : CARRIERS DENSITY



FDSOI MOSFET RESULTS



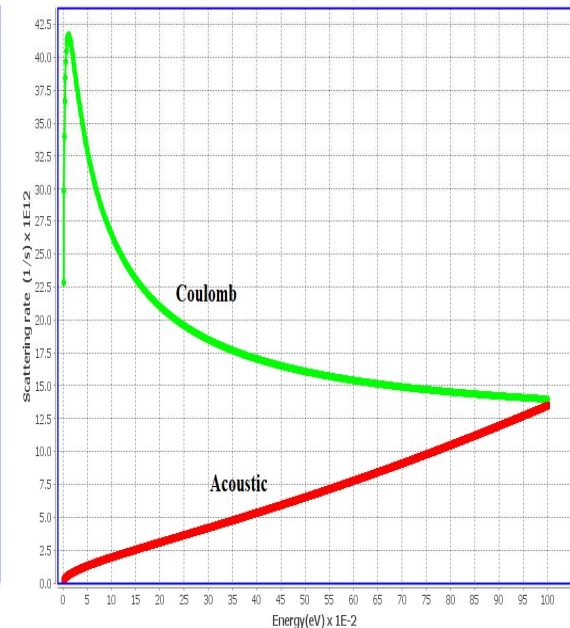
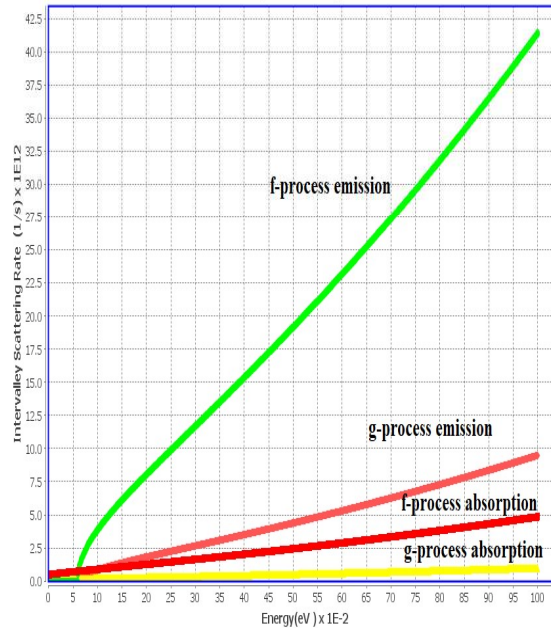
Structure Parameters	Nodes (nm)	14nm	10nm	7nm	14nm	10nm	7nm
		Single Gate			Double Gate		
L_{eff} (nm)	22	14	10	22	14	10	
W_{eff} (nm)	10	8	10	8	10	8	
T_{ox} (nm)	1	0.85	0.75	0.75	0.85	0.75	
Doping (/cm ³)	1×10^{24}	5×10^{24}	2×10^{25}	2×10^{25}	5×10^{24}	2×10^{25}	
T_{SOI} (nm)	40	30	20	20	30	20	
Device Parameters	V_{th} (mV)	0.3	0.22	0.2	0.2	0.4	0.5
	SS (/mV/dec)	63.3	67.9	82.9	82.9	87.4	72.2
	gm (mS/ μ m)	0.252	0.437	0.499	0.499	0.494	0.449

FDSOI TECHNOLOGY UP TO 7NM



Scattering Rates

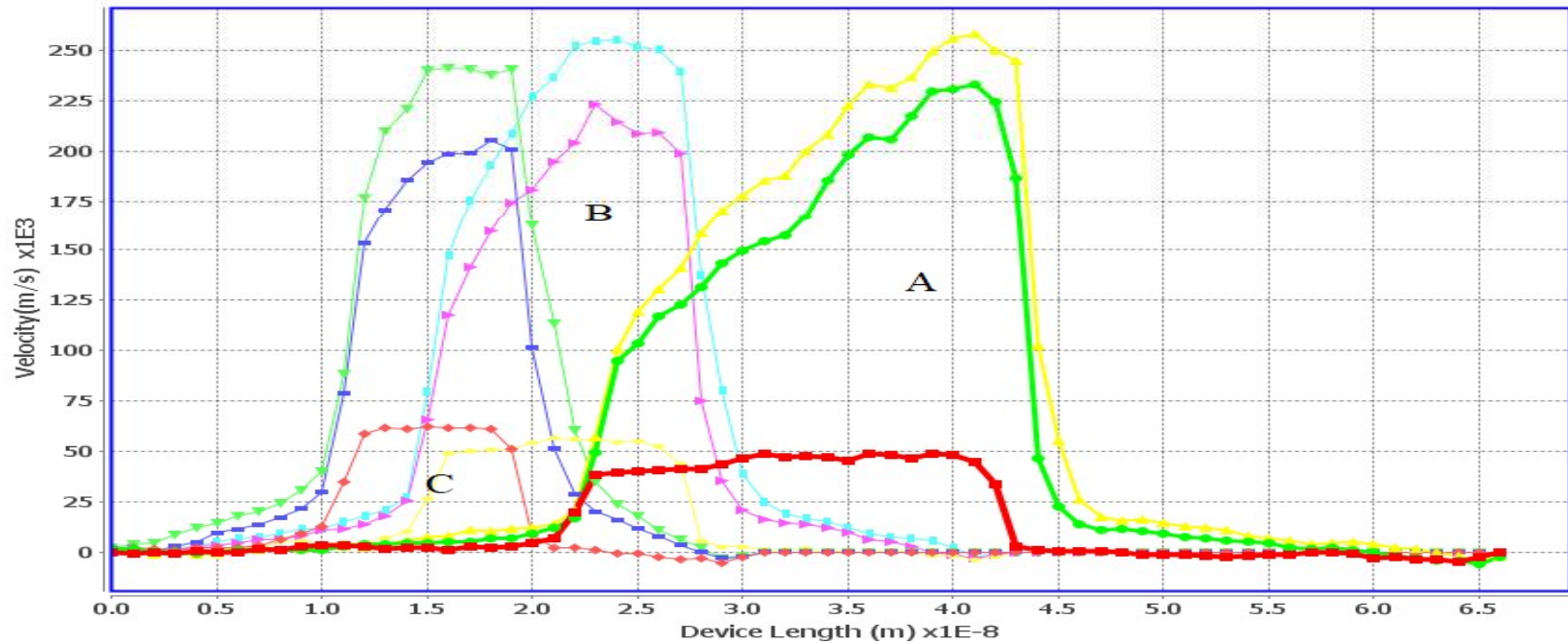
- Intervalley,
- Acoustic and
- Coulomb



DRIFT VELOCITY

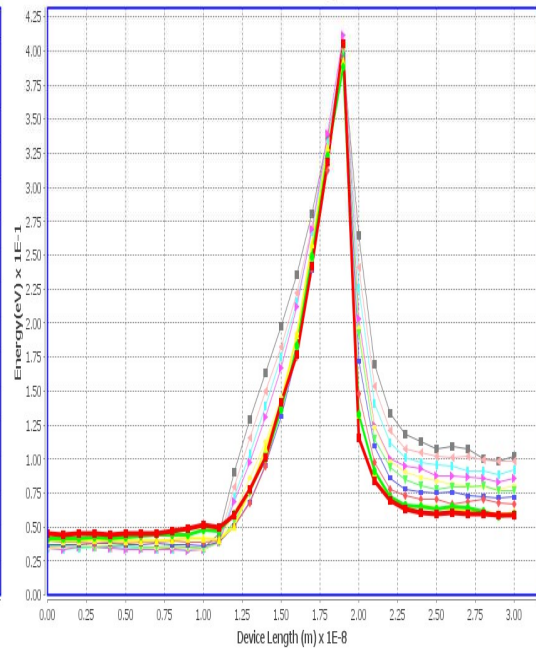
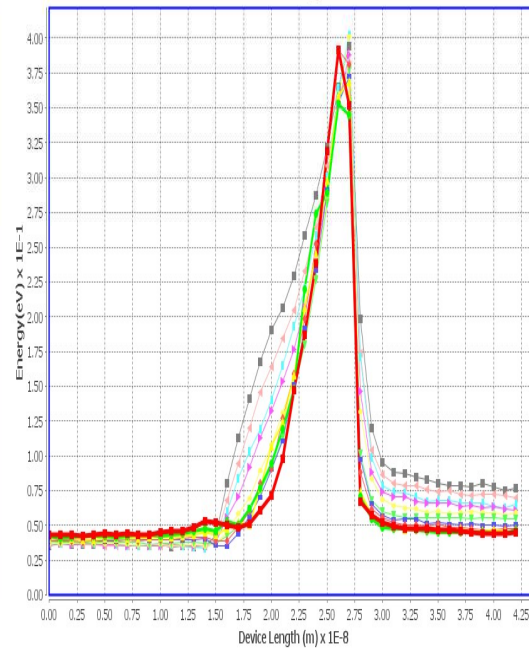
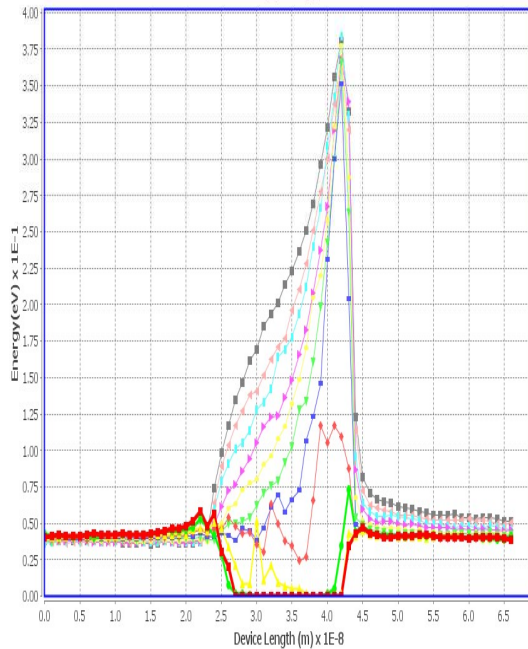


Carrier Drift Velocity for 7nm, 10nm and 14nm (Back Gate off)



Carrier Drift velocity a) 14nm b) 10nm c) 7nm

CARRIER AVERAGE ENERGY

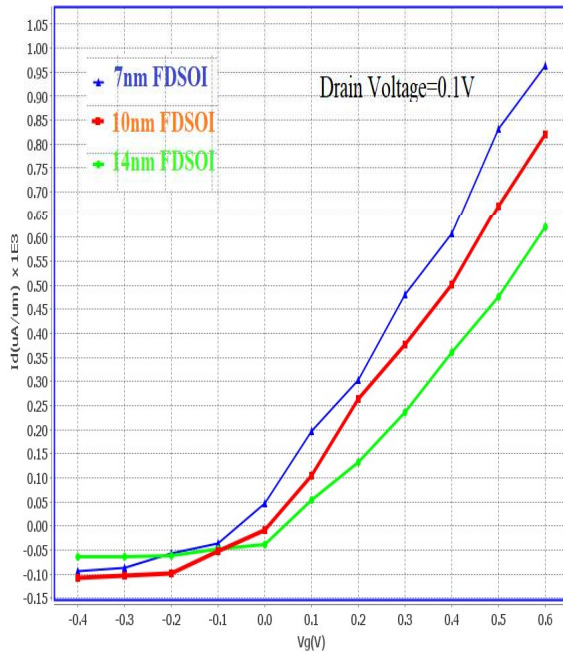


a) 14nm FDSOI MOSFET b) 10nm FDSOI MOSFET c) 7nm FDSOI MOSFET

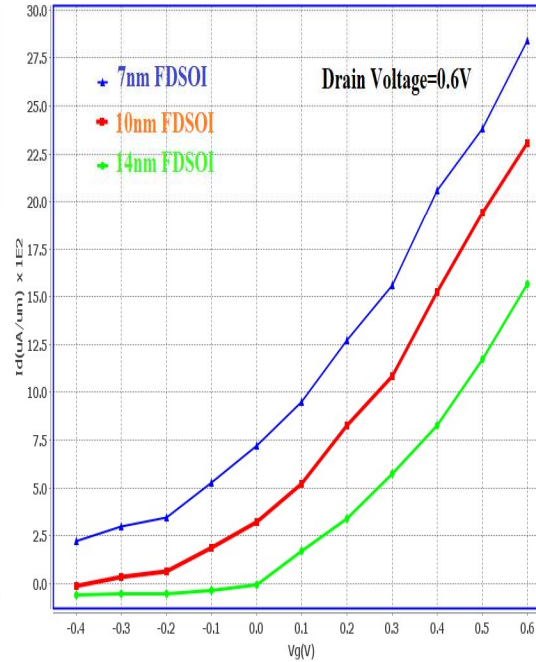
Transfer $I_d - V_{g_s}$ Characteristics



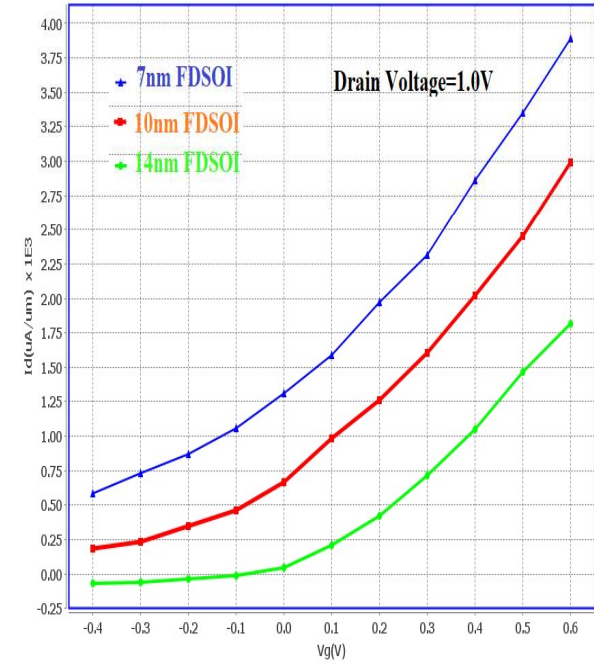
I_V_Characteristic



I_V_Characteristic



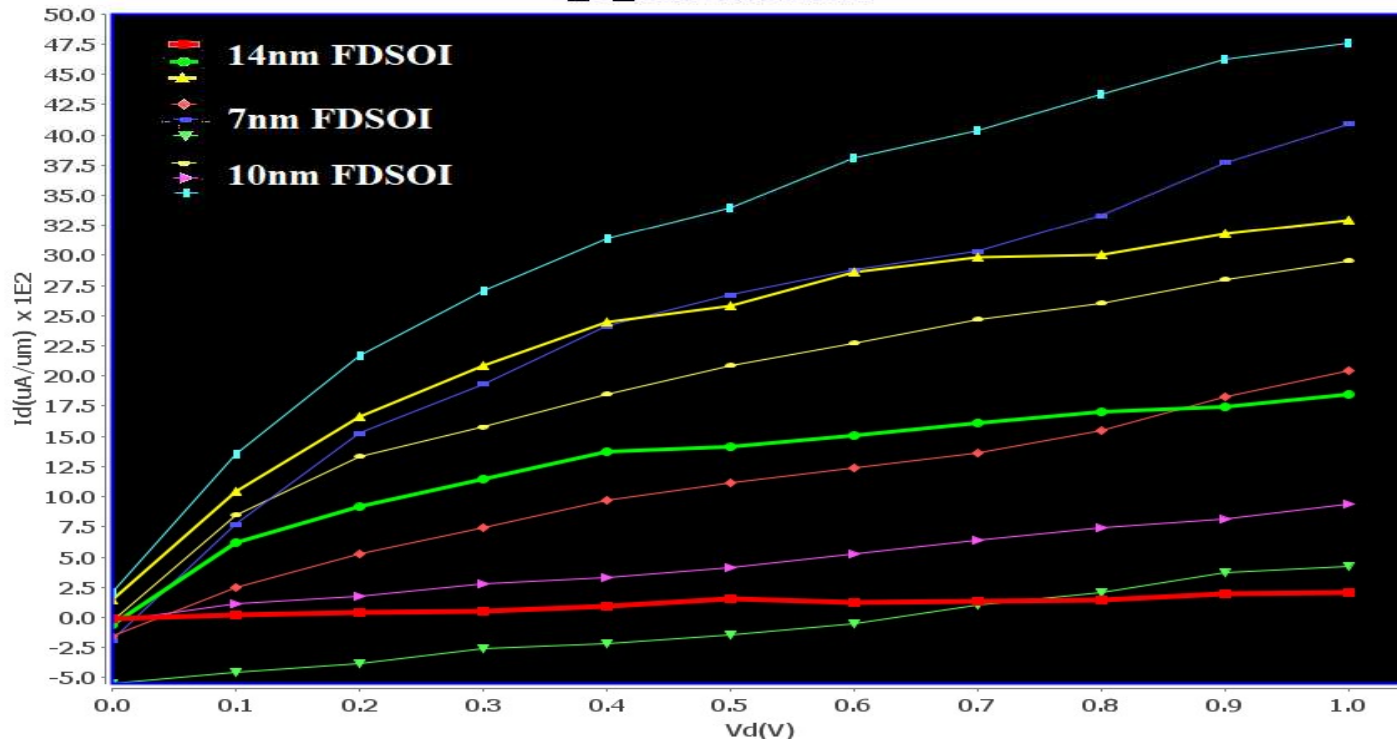
I_V_Characteristic



Single Gate $I_d - V_d$ Characteristics



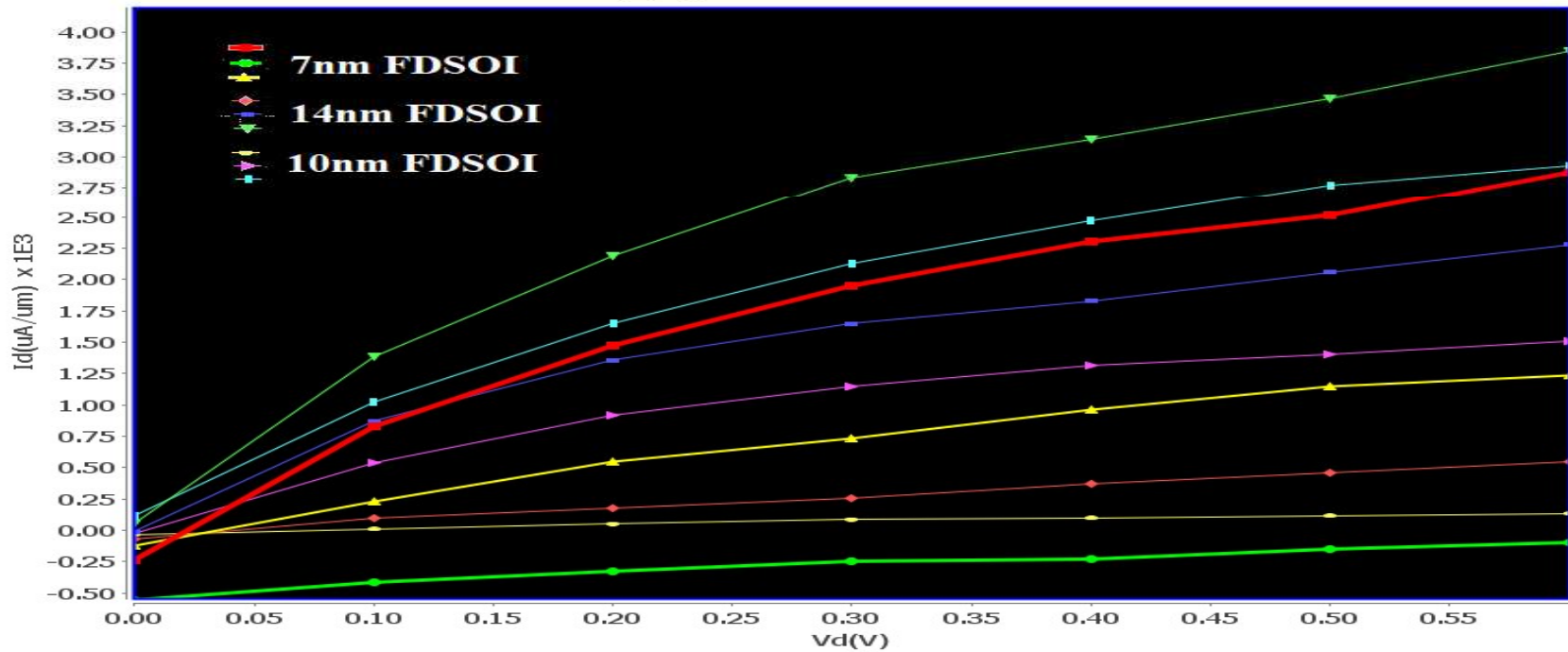
I_V_Characteristic



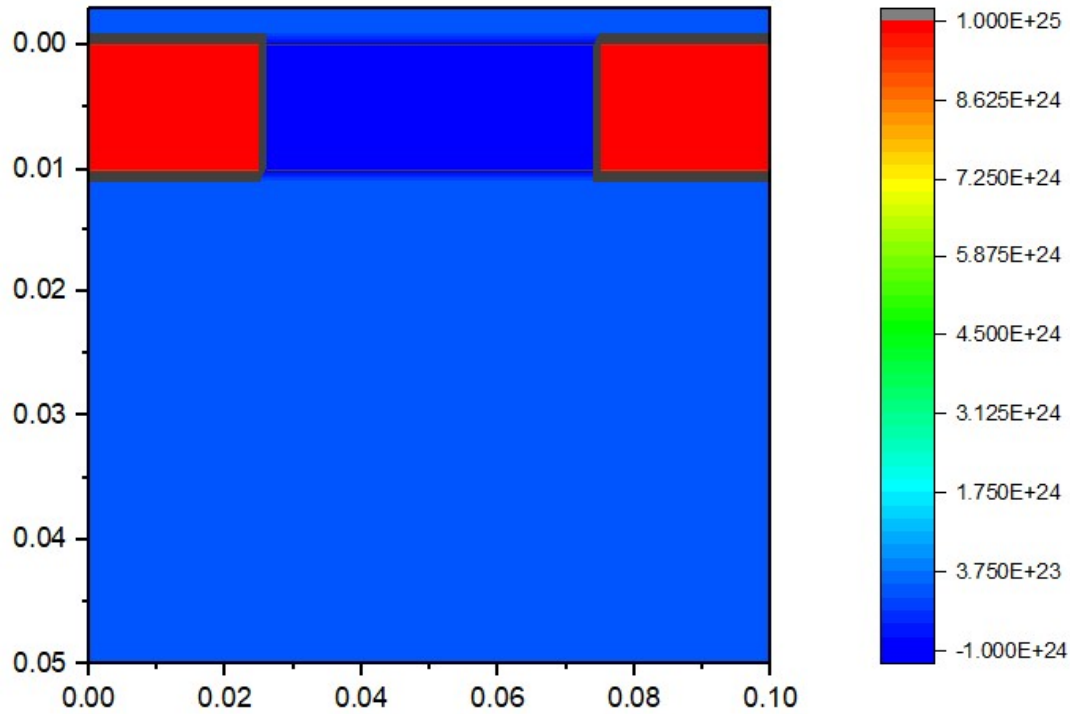
Dual Gate $I_d - V_d$ Characteristics



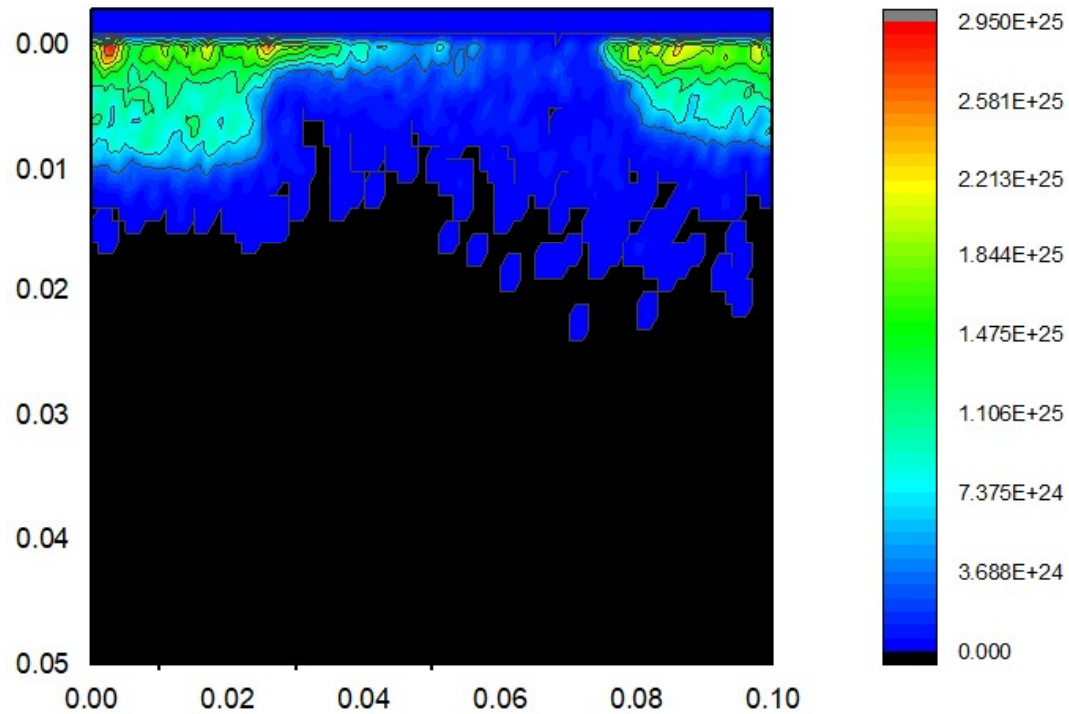
I_V_Characteristic



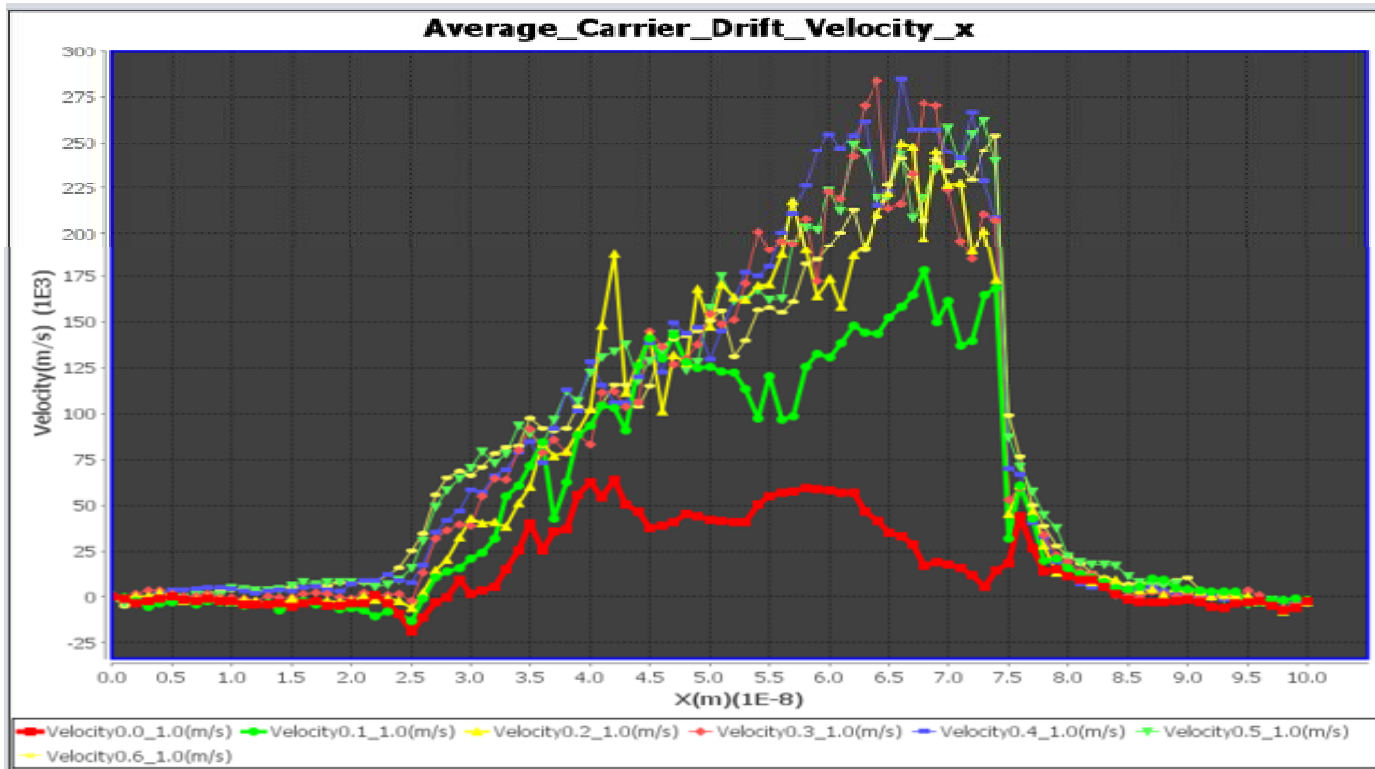
MOSFET



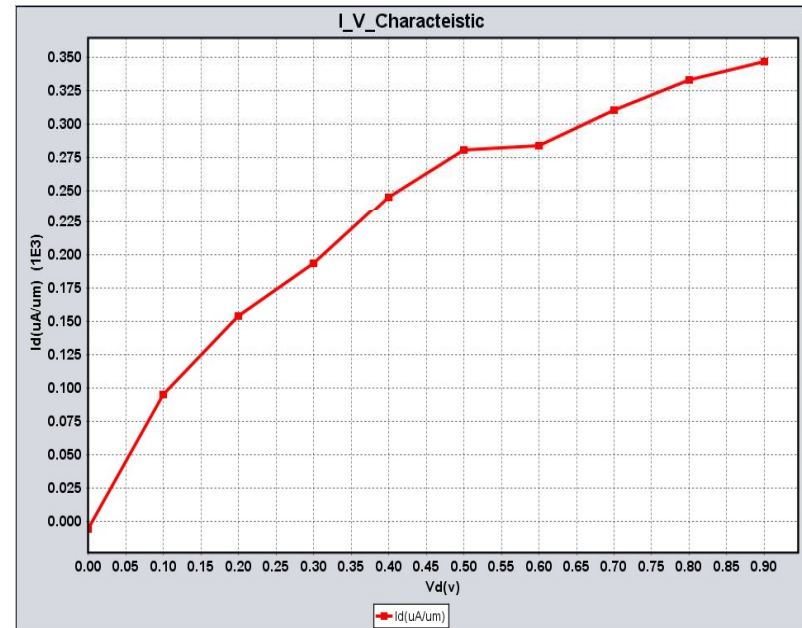
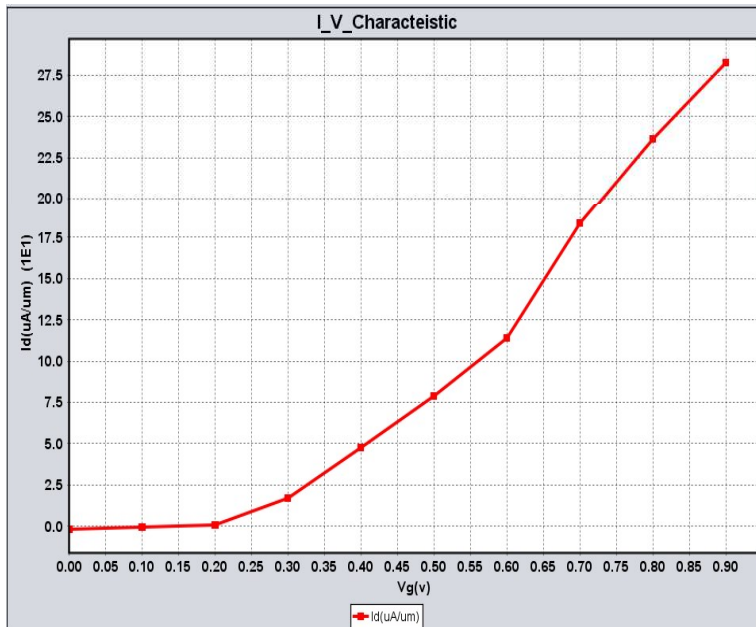
MOSFET: Carrier Density



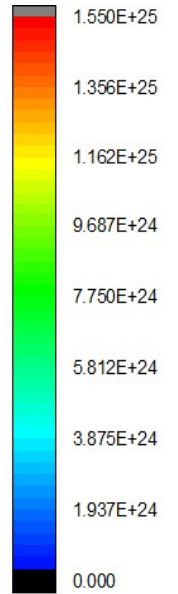
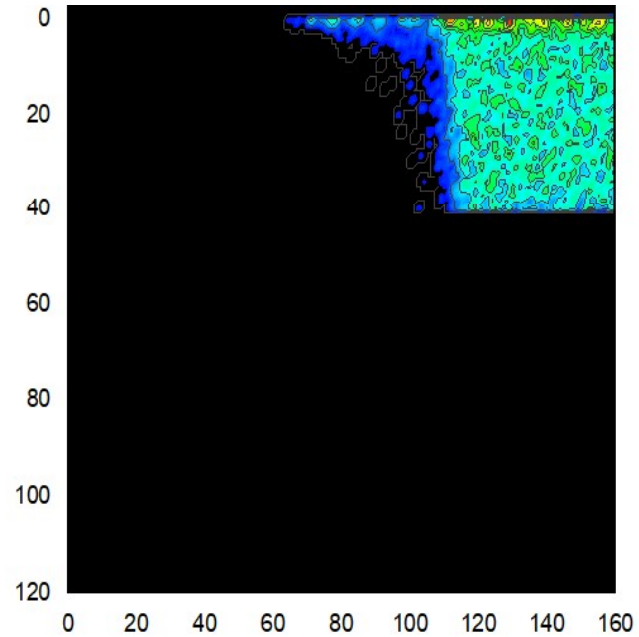
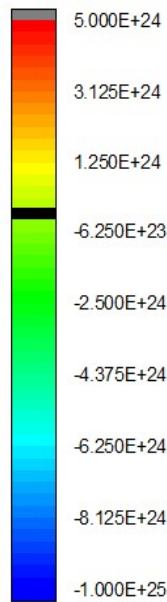
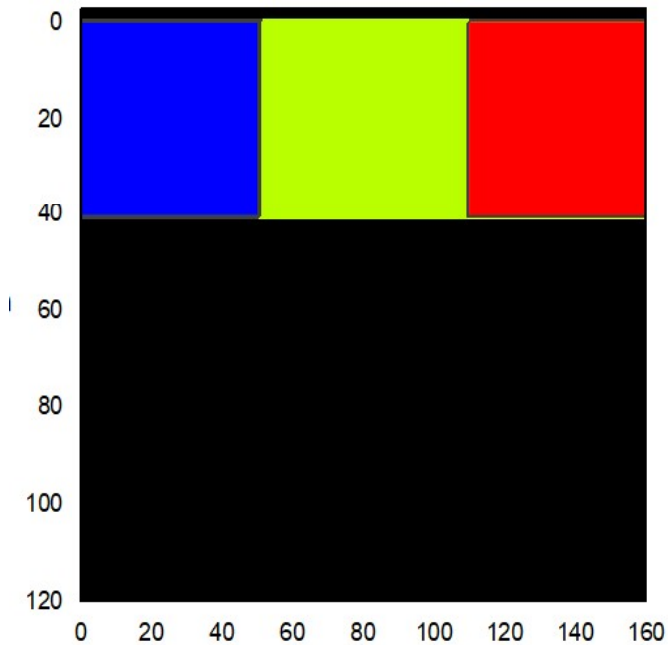
MOSFET: Carrier Drift Velocity



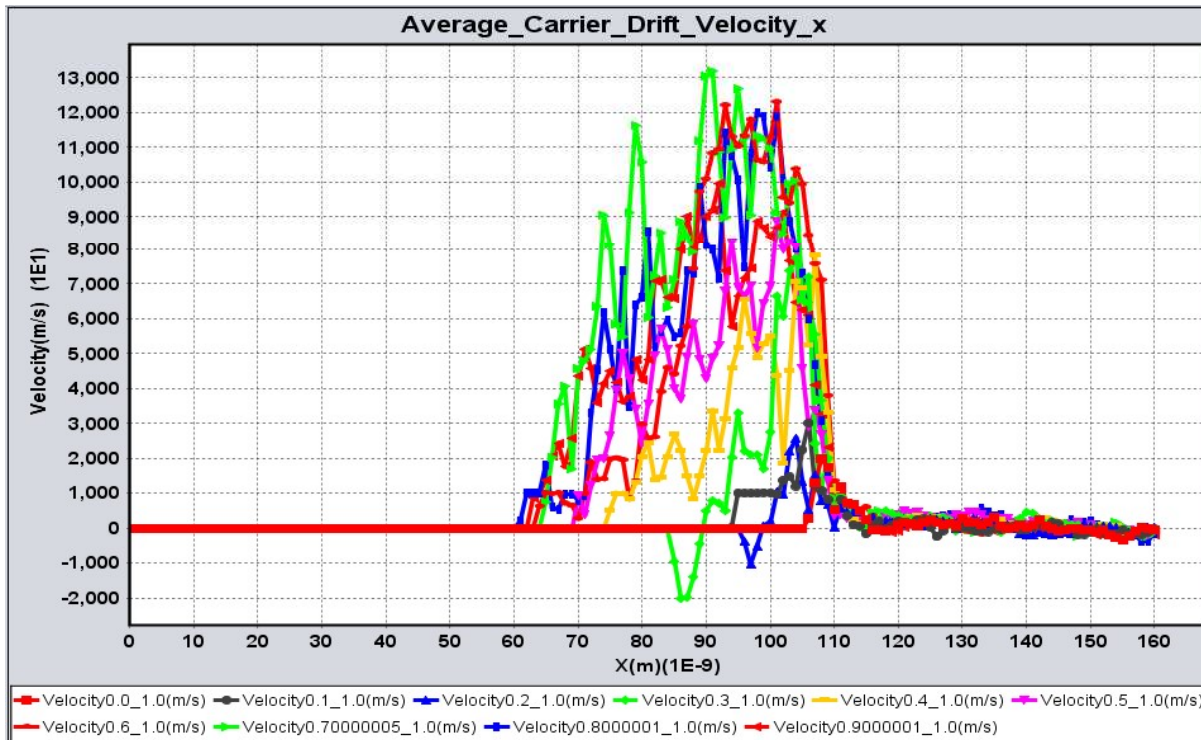
MOSFET Transfer Characteristics



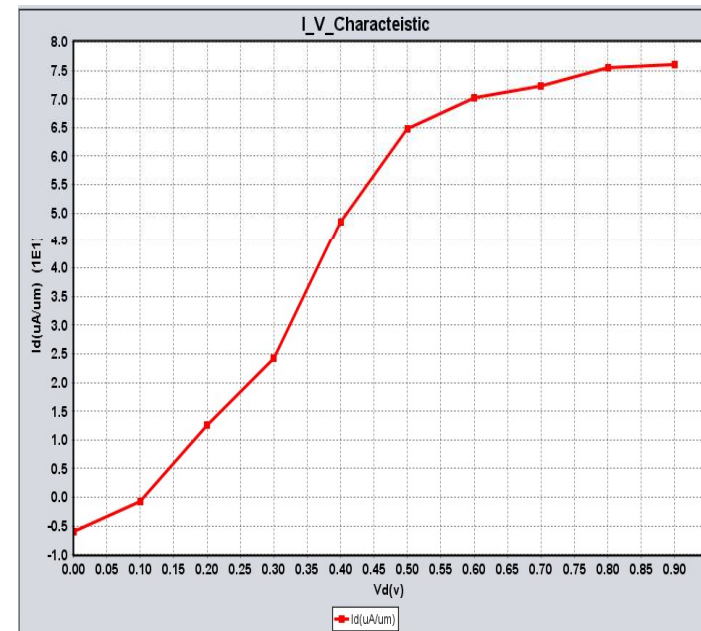
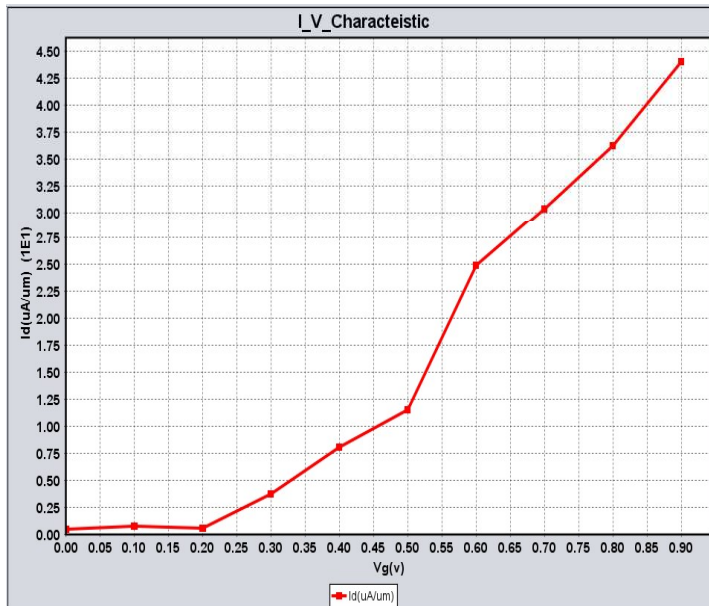
Tunneling FET



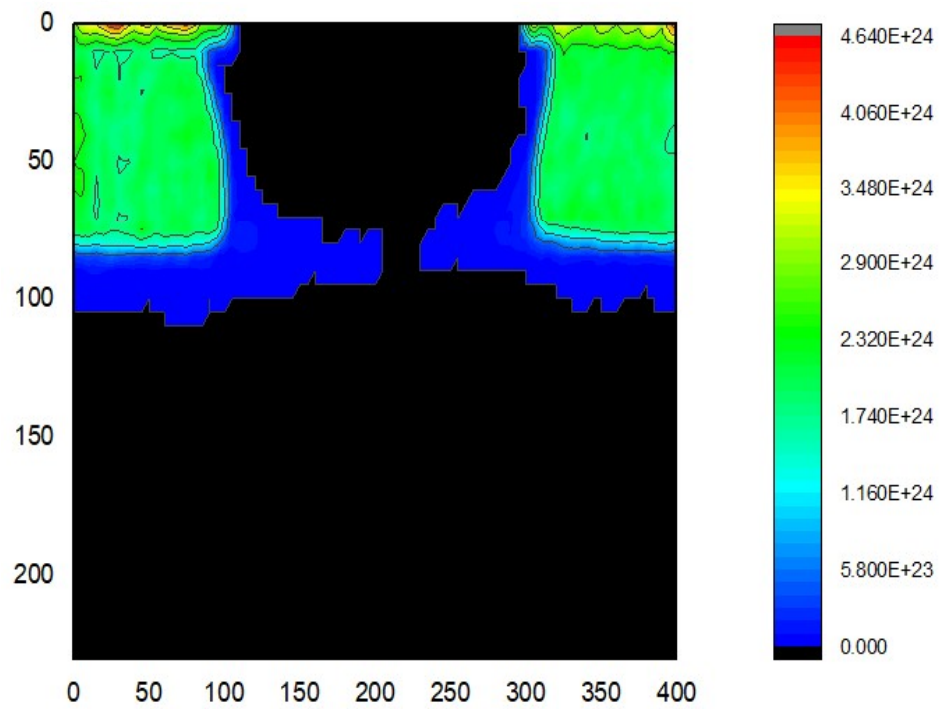
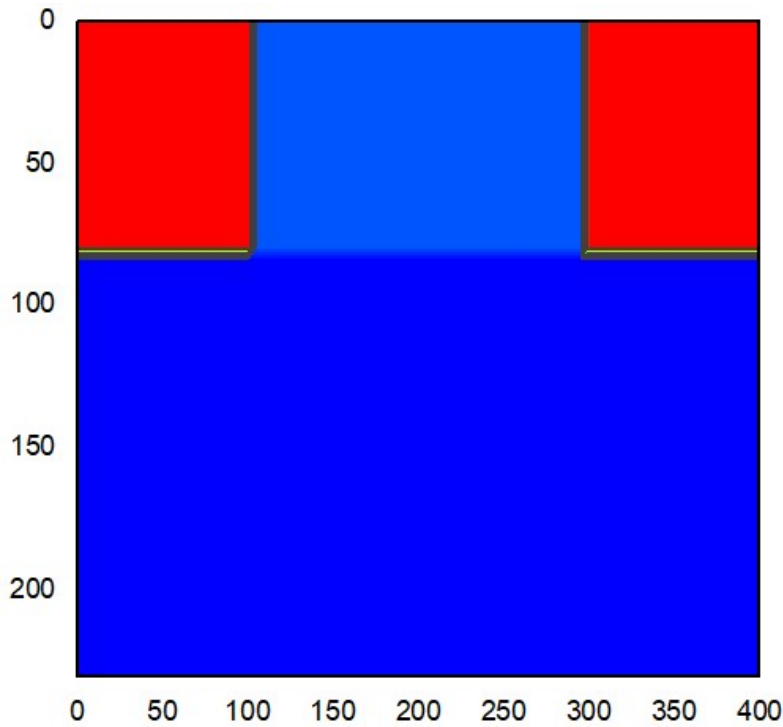
Tunneling FET



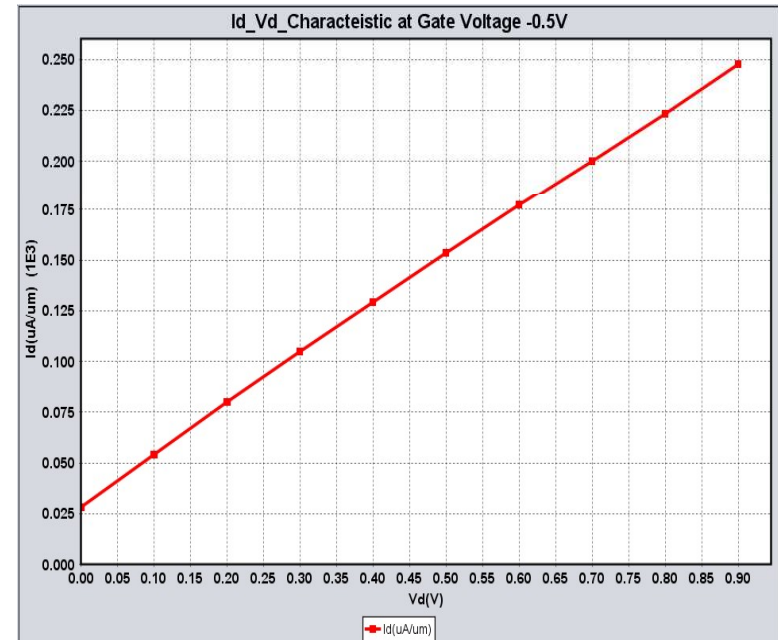
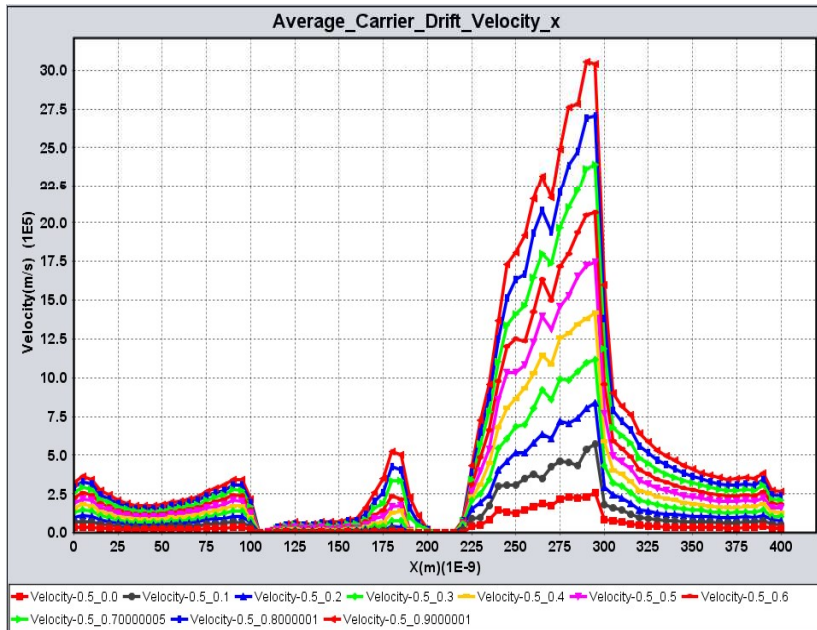
Tunneling FET Transfer Characteristics



MESFET



MESFET



ADVANCE LICENSING & PRICE VALUE



TNL's tools support advanced and unique licensing models tailored for unique customer needs.

➤ **ADVANCED LICENSING OPTIONS:**

- Term-Based
- Perpetual
- TCAD Academic Suite
- 24x7 Technical Support for **Academic Institutions**

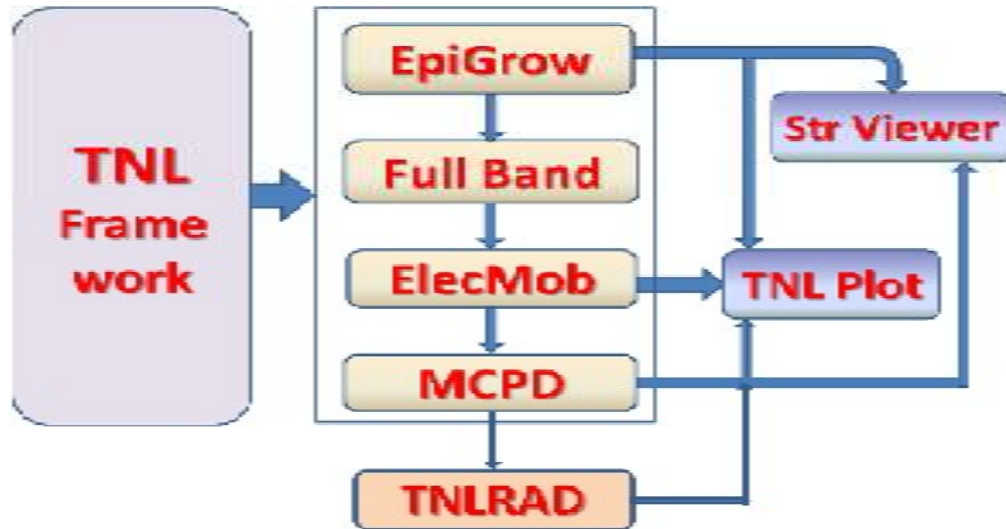


Publications



1. P.K. Saxena, numerical study of dual band (MW/LW) ir detector for Performance improvement, *Defence Science Journal*, vol. 67(2), (2017) pp. 141-148. DOI : 10.14429/dsj.67.11177
2. Praveen K. Saxena, Pankaj Srivastava, R. Trigunayat, An innovative approach for controlled epitaxial growth of GaAs in real MOCVD reactor environment, *Journal of Alloys and Compounds*, vol. 809 (2019) 151752. <https://doi.org/10.1016/j.jallcom.2019.151752>
3. Praveen Saxena, R. Trigunayat, Anchal Srivastava, Pankaj Srivastava, Md. Zain, R.K. Shukla, Nishant Kumar, Shivendra Tripathi, FULL ELECTRONIC BAND STURCTURE ANALYSIS OF Cd DOPED ZnO THIN FILMS DEPOSITED BY SOL-GEL SPIN COATING METHOD , II-VI US Workshop Proceedings, 2019.
4. R. K. Nanda, E. Mohapatra, T. P. Dash, P. Saxena, P. Srivastava, R. Trigutnayt, C. K. Maiti, Atomistic Level Process to Device Simulation of GaNFET Using TNL TCAD Tools, [Advances in Electrical Control and Signal Systems](https://doi.org/10.1007/978-981-15-5262-5_61) pp 815-826, (2020), Springer Book. https://doi.org/10.1007/978-981-15-5262-5_61
5. Sanjeev Tyagi, P. K. Saxena, Rishabh Kumar, Numerical simulation of $\text{In}_x\text{Ga}_{1-x}\text{As}/\text{InP}$ PIN photodetector for optimum performance at 298 K, *Optical and Quantum Electronics* (2020) 52:374. <https://doi.org/10.1007/s11082-020-02488-1>
6. Praveen K Saxena *at. el.*, An Innovative Model for Electronic Band Structure Analysis of doped and un-doped ZnO, *Journal of Electronic Materials* Accepted for publication.
7. Anshika Srivastava, Anshu Saxena, Praveen K. Saxena, F. K.Gupta, Priyanka Shakya, *at. el.*, An innovative technique for electronic transport model of group-III nitrides, [Scientific Reports nature research](https://doi.org/10.1038/s41598-020-18706-8) (2020) 10:18706.

ATOMISTIC TCAD TOOLS



- Epitaxial Growth Process
- Material Characterization
- Material Characterization
- Particle based Device
- Impact of Radiation / High Frequency EM waves (under Development)



Thank You
Contact us



+91-983-915-1284



info@technextlab.com



Lucknow 226 003, INDIA



www.technextlab.com

